UNITED NATIONS UNIVERSITY
GEOTHERMAL TRAINING PROGRAMME
Orkustofnun, Grensásvegur 9,
IS-108 Reykjavík, Iceland

Reports 2008
Number 23

BOREHOLE GEOPHYSICS AND GEOLOGY OF WELL H-43, LOS HUMEROS GEOTHERMAL FIELD, PUEBLA, MÉXICO

Cecilia Dolores Lorenzo Pulido
Comision Federal de Electricidad (C.F.E.)
Geothermal Projects Management
Alejandro Volta 655, Col. Electricistas
Morelia, Michoacán de Ocampo
MEXICO
cecilia.lorenzo@cfe.gob.mx

ABSTRACT

This report is about the geology, seismic and electromagnetic surveys, drilling operations and borehole geophysical logging of well H-43, located within the Los Humeros geothermal field in Puebla, México. Data acquisition and preliminary interpretations from the drilling operation include the description of drill-cuttings, lithology, alteration and geophysical logging, including data from a Fullbore Formation MicroImager (FMI). Drilling operations were conducted by the Mexican company LATINA. Data acquisition was conducted by the Comision Federal de Electricidad (C.F.E.) and Schlumberger. Well H-43 was spudded on October 22nd, 2007 with drill rig IDECO 2 and was drilled down to a depth of 2200 m. Well operations were concluded on January 7th, 2008. The information was analyzed to identify possible fracture systems in the well in relation to the different rock units and feed zones. The interpretation of temperature data shows that well H-43 is a high-temperature well (maximum temperature recorded is 395.4°C). A petrographic analysis identified the well as being acidic, mostly observed in the rock formation. FMI and breakout parameters were interpreted. Different fracture and fault zones were identified in the well with a main fracture dip at 50-60°, and up to 80° for fault zones. The preferential strike directions for fracture and fault zones lie between N-S and NNE-SSW. These fault zones are consistent with field observations and the Antigua fault strike direction. Well H-43 is a potential production well with an estimated fluid output of 51.95 tons/h.

1. INTRODUCTION

Mexico is located in Middle America, bordering the Caribbean Sea and the Gulf of Mexico to the east, between Belize and the USA, and bordering the North Pacific Ocean to the west, between Guatemala and the USA. All of Mexico is located within an active zone of volcanism and tectonics with its main land being part of the North American Plate. The country contains the Baja California Peninsula and the Cocos Plates in the northwest and along the Pacific coast, and the Trans-Mexican volcanic belt that stretches in an east-west direction over the southern part of the country (see Figure 1). The Trans-Mexican volcanic belt includes the main focus area of this report, the Los Humeros geothermal field.

The Los Humeros volcanic system is the easternmost of a series of silicic volcanic centres with active geothermal systems located north of the axis of the Mexican volcanic belt with a summit elevation of

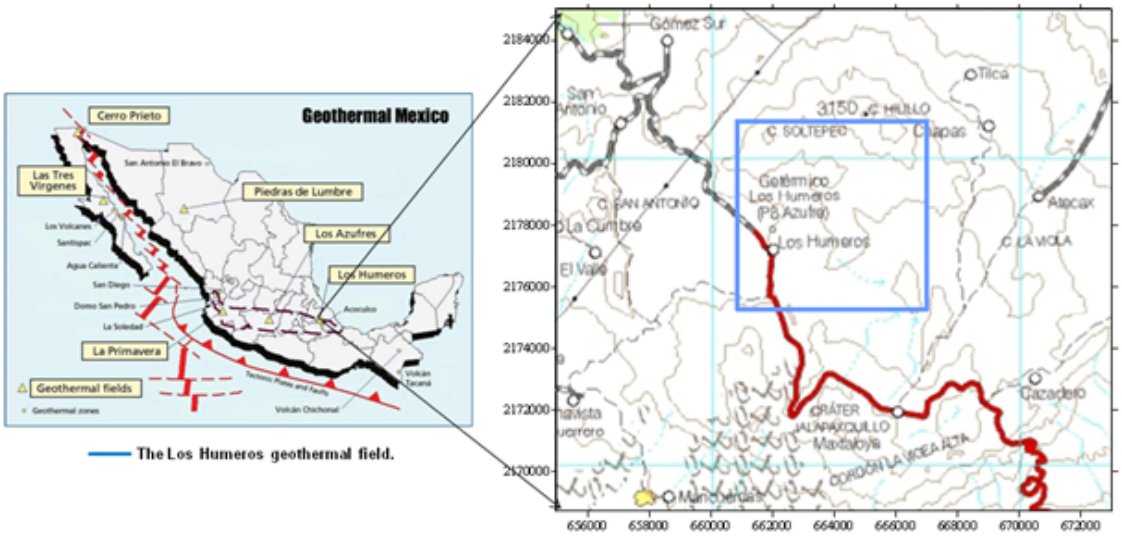

FIGURE 1: Geothermal zones of Mexico and the location of the Los Humeros field

3150 m, latitude 19.68°N and longitude 97.45° W (see Figure 1). The first major silicic eruption produced the 230 km^3 Xáltipan ignimbrite about 460,000 years before present (BP), which covered about 3500 km^2 and resulted in the formation of the 15×21 km^2 Los Humeros caldera. The developments of post-caldera lava domes and eruptions of the 40 km^3 Faby tuff about 240,000 years BP were followed by eruptions that formed the Zaragoza tuff formation about 100,000 years BP that marks the formation of the nested 10-km-wide Los Potreros caldera. A third and much smaller caldera (El Xalapazco) was formed approximately between 40,000 and 20,000 years BP. The most recent eruptions with extensive basaltic lava flows at the Los Humeros volcanic system formed the existing surface morphology of the area. The basaltic lava flows are undated, but are estimated to be younger than the 20,000 years BP dated rhyolitic lava flows and could have originated in part in early Holocene age (Negendank et al., 1985). Hot springs and active fumaroles are still present at Los Humeros to this day. Geologic interpretations of structural, geophysical, and drilling data suggest that:

1) The water-dominated geothermal reservoir is hosted by the earliest andesitic volcanic formation that is bound by the ring-fracture zone of the Los Potreros caldera, and is covered by the deposits of the oldest caldera-forming eruption;
2) Permeability within the andesitic formation is provided by faults and fractures that are related to intra-caldera uplift;
3) The geothermal system has a potential for a large influx of meteoric water through parts of the ring-fracture zones of both calderas.

The Los Humeros geothermal field (Figure 2) is the second geothermal field in the Mexican volcanic belt to be developed; the first is the Los Azufres geothermal field, 90 km east of Morelia (Figure 1). The Los Humeros field has an installed capacity of 40 MWe (eight back-pressure units of 5 MWe net each) and produces from 20 wells. Separated brine is completely injected back into the reservoir through 3 injection wells. The total installed geothermal capacity in Mexico reaches 958 MWe at present.

2. GEOLOGICAL STUDIES

Existing and ongoing regional and field scale geological studies and data permit a good overview of the internal formations and structures of the subsurface at the Los Humeros geothermal field area. Using all geological and geophysical information, a new drill site needs to be located and developed to help supply additional steam for the growing energy demand.

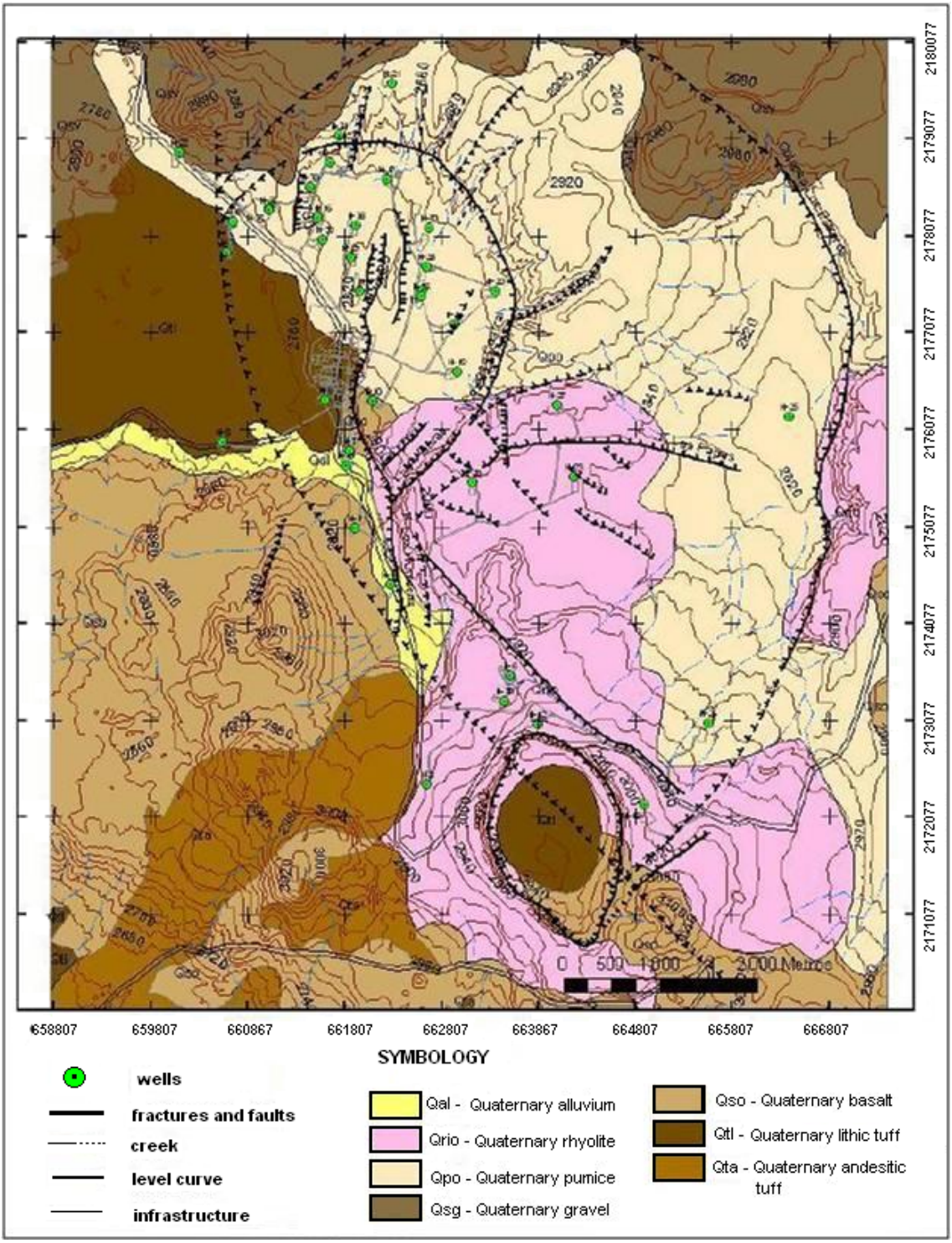

FIGURE 2: Local geology of the Los Humeros geothermal field

2.1 Local geology

The currently exploited Los Humeros geothermal field is located in a volcanic structure within the Los Humeros caldera (Figure 2). Locally obtained and analyzed structural surface data in the field indicate that the main present fracture systems strike NW-SE, N-S and also a few NE-SW. Of special note is the geometry of the Maztaloya fault, as its N-S strike direction was confirmed using these surface observations. With additional field data, it was also possible to detect that thermal manifestations primarily follow the N-S orientated fault systems (Rocha et al., 2006).

The Los Humeros geothermal field has a complex geologic structure with a fluid flow controlled by fracturing. It has been speculated that observed narrow elongated zones of seismicity may be due to stress releases caused by fluid flow (Boyle et al., 2007) (see Figure 3).

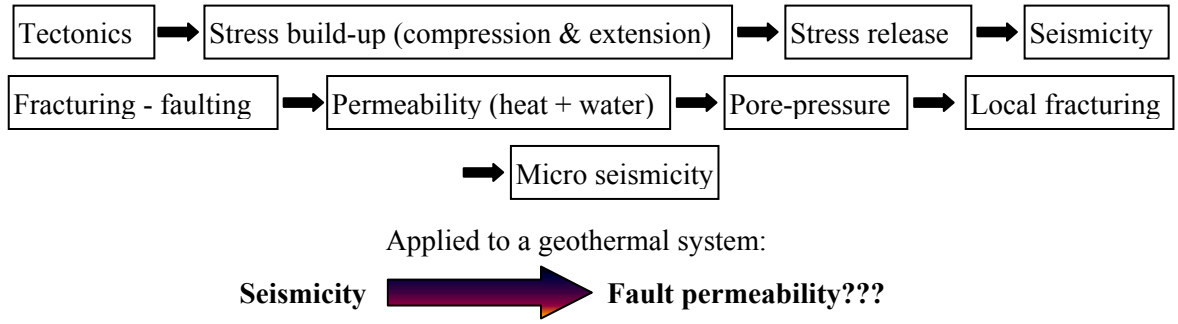

FIGURE 3: Correlation between seismicity and stress release caused by fluid flow

2.2 Volcanology

The volcanic activities in the Los Humeros field area occurred during the Neogene period. It is possible to group these activities into three episodes in accordance with the lithologic descriptions of the borehole data:

1. The volcanic activities of the Upper Miocene (10.5 Ma) are characteristic for the andesites-hornblende formation called Cuyuaco. Fractures and geological fault zones generally present the main reservoirs. The andesites are the first overlying volcanic deposits on top of the basement, which consists of marls and limestones. These volcanic deposits are a series of tuff formations, which are mixtures of rhyolitic tuffs and Ixtacacamaxtitlan tuffs, and are associated with the intrusion of rhyolitic domes into the basement.

2. The volcanic activities of the Pliocene (1.5-5 Ma) are represented by the andesites of augite Teziutlan formation with gross-thicknesses between 600 and 1100 m, and with alternating deposits of tuffs and ignimbrites. These deposits can be interpreted as the stratovolcano interval of the pre-caldera structures of the Los Humeros region. The Teziutlan formation, consisting of augite rich andesites, contains the geothermal reservoirs.

3. The Plio-Quaternary volcanic activities (Pleistocene-Holocene) have an explosive character with calderic and post-calderic episodes at Los Humeros and Los Potreros. The first phase was the result of a Plinian eruption with explosive deposits of approximately 15 km^3 of Xaltipan ignimbrite of rhyolitic composition (0.46 Ma ago). The collapse of the caldera was marked by a Plinian eruption with associated fissures and deposits, such as lithic tuffs, rhyolitic domes, ashes, andesite domes, and olivine basalt flows and scoria that have been dated as old as 0.24 Ma and as young as 0.02 Ma.

2.2.1 Intrusive igneous activity

The final stages of the Laramidic Orogenic caused the sedimentary calcareous basement to shear and break. Through zones of weak and deep reaching faults systems, the rising of intrusive bodies such as grain-dioritic intrusions, micro-granite intrusions and sienite intrusions was possible, primarily formed by stock-like intrusions. This is fairly well confirmed by the degree of contact-metamorphism of the sedimentary basement rock, where contacts such as skarn, hornfels and marmor marble were recorded. The dating in these intrusive rocks indicates an age between 31 Ma and 14 Ma within the Lower Oligocene to Middle Miocene.

2.3 Regional structural geology

The geological structure of the Los Humeros field has been studied on a regional scale (tectonic), from Jurassic to the present. In particular, an attempt was made to locally explain the interrelations of lithological units and their possible geometry.

The studies indicate that the limestones of the Cretaceous lower Tamaulipas formation are located right below the volcanic belt. These limestone sequences are part of the Mexican Huayacocotla thrust belt that was created during the Late Cretaceous Laramide orogeny.

Well observations have shown that a structural high exists for the area around wells H-2 and H-5, which cut limestone of Jurassic age at 1140 m in wells H-2 and 1370 m in well H-5. The top of that shallow structural high appears to correspond with the front folds and recumbent folds of the Huayacocotla thrust belt. On the other hand, well observations indicated structurally low areas around wells H-4, H-7, H-12 where the top of the lower Tamaulipas limestone formation was not reached and the deposits of volcanic rocks of the Neogene period appear to exceed a depth of 2500 m.

The first compression episode at the end of the Cretaceous time affected the sedimentary sequences and is characterized by ductile deformation during the Laramide orogeny with its direction of maximum stress ($\sigma 1$) of N40°E. This compression resulted in the forming of anticlines and recumbent folds and created the inverse faults of the Sierra Madre Oriental, the highest structural area of the region that showed strike directions between N10°W and N40°W. Not all stages of distortion that lower Tamaulipas sequence experienced thereafter have been described – but it is not possible to ignore the stage of rock distortions caused by the Lower Oligocene to Middle Miocene intrusions that introduced a trans-tensional stress regime to the rock formations. In the structurally high located areas in the region, e.g. around wells H-2 and H-5, sets of normal faults most likely formed during that time. These fault sets strike NW-SE and N-S with a general dip direction due east and most likely reach the uppermost crust. Examples for these fault zones are the Antigua- and possibly Malpais fault zones, where volcanic intrusions were found associated with the fault sets.

The second stage of structural deformation in the area is described as trans-tensional, principally caused by the three volcanic cycles of the Mexican volcanic belt from the Tertiary to Quaternary. To this day, no clear structural sub-surface interpretation exists, that could show the three-dimensional morphology of the structures and formations of the Los Humeros caldera. Consequently, precise fault and fracture zone locations in a three-dimensional interpretation are missing.

The deep andesitic formation, interpreted based on core and cutting samples of well H-43, suggests a possible correlation with the Cuyuaco andesite (10.5 Ma) formation of the Upper Miocene. This andesite is much fractured and presents the main geothermal reservoir. This has been interpreted to be related to tectonic extension activities that began around the Pliocene (Upper Tertiary). This extension caused the forming of extensive fracture and fault systems that later coincided with the emission of the lava flows. At first, the fault and fracture systems showed a general strike direction between N20°W and N70°W, but later changed direction to a system striking between N and N20°E and a younger stage of re-activation of these structures. These youngest fault and fracture systems are associated with geothermal manifestations, such as zones of hydrothermal alteration and lineaments of volcanic centres that define them as conductive structures for heat flow (e.g. Mastaloya system, the La Cuesta fault and the Loma Blanca fault), which connected the lowermost volcanic units to the Cuyuaco andesite containing vitric tuffs, andesites of augite and possibly the Xaltipan ignimbrites.

The presence of intrusive granitic bodies and biotite rich micro-grain dioritic intrusions are part of an intrusive system that was active during the trans-tensional phase and caused metamorphism, e.g. skarns and metamorphism of the limestone sediments into marble. There has been evidence that the Cuyuaco lavas metamorphed the surrounding strata.

3. GEOPHYSICAL STUDIES

The Los Humeros geothermal field has been the object of a large number of geophysical studies. The objective of these studies was to visualize and interpret the physical properties of the subsurface and its relationship with thermally active zones. The geophysical studies that have been conducted include:

- Vertical electrical soundings;
- Transient Electromagnetics (TEM);
- Gravimetric surveys;
- Reflection seismic surveys;
- Passive seismic studies (seismic monitoring).

3.1 Vertical electrical soundings

The vertical electrical soundings revealed two important anomalies of less than 80 ohm-m (Figure 4). One of them defines the horizon of the andesites and the secondary sequence (limestone), between 600 and 800 metres above sea level (m a.s.l.), corresponding to the producing zone of hydrothermal alteration; the other anomaly lies between 1000 and 1800 m a.s.l., where, based on information from wells near H-43, there must exist zones contributing to high-temperature fluids in the igneous volcanic rocks (andesite) (Palma, 2007). Temperature logs were done in production wells H-33 and H-16 and high temperatures recorded, as can be seen in Table 1.

TABLE 1: Maximum temperatures recorded in production wells H-33 and H-16

H-33		H-16	
Location (m a.s.l.)	**Temp. max. (°C)**	**Location (m a.s.l.)**	**Temp. max. (°C)**
1350	251	1350	213
		700-1050	269

Production well H-16 (elevation 2783 m) was drilled through a semi-resistive anomaly (59-85 ohm-m) that is associated with the andesite formation. Production well H-33 (elevation 2782 m) identified one small part of the La Cuesta fault at 1400 m depth.

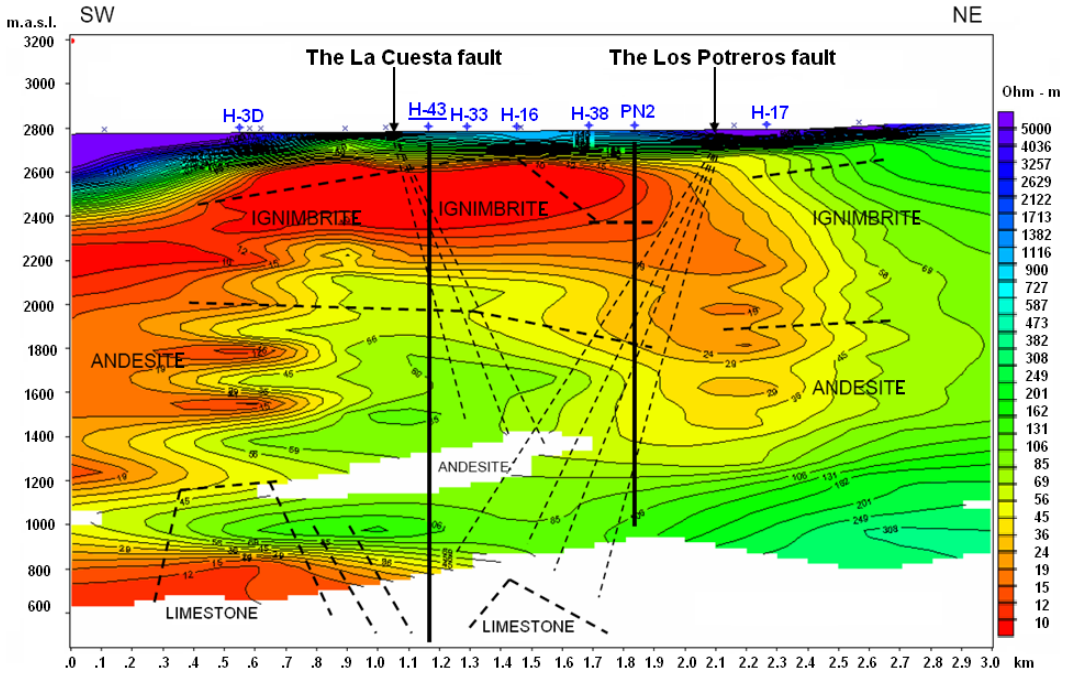

FIGURE 4: Vertical electrical soundings cross-section (by Palma, 2007); white indicates that data is not available

3.2 TEM

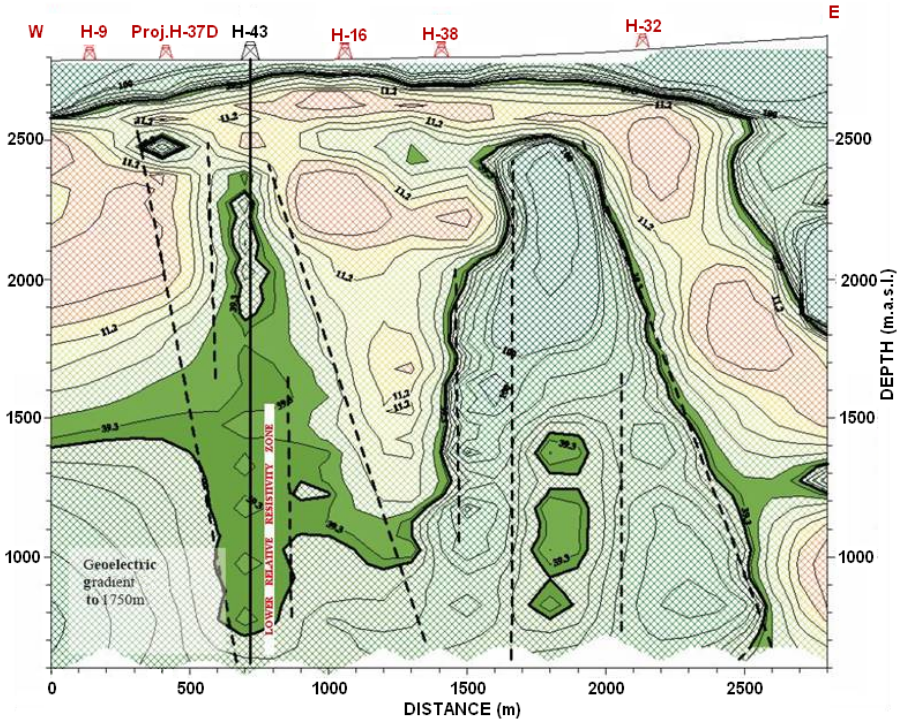

FIGURE 5: Cross-section from TEM soundings in the Los Humeros field (by Palma, 2007)

The analysis and interpretation of the TEM soundings revealed the following: A resistivity anomaly of 40 ohm-m of vertical elongation is seen from 500 to 2000 m depth (Figure 5). A resistive formation of 80 ohm-m indicates a discontinuity associated with a volcanic body and the limestone basement, located approximately between 1750 and 2200 m depth. This resistivity anomaly relates to a thermal anomaly where high temperatures are or have been prevailing. Furthermore, this anomaly is associated with zones of high hydrothermal alteration, where the fluids with the highest temperature are produced (Palma, 2007).

3.3 Gravimetric and reflection seismic surveys

By means of the gravimetric and reflection seismic surveys, it was interpreted that the top of the sedimentary rocks would be at a depth of 2000 m. However, the well reached these at 1740 m depth, i.e. with a 13% error in the estimation. The seismic reflection method used is considered to provide an estimate of depths with ±10% error (Rocha et al., 2006).

3.4 Passive seismic studies

Information from active seismicity in the Los Humeros geothermal field has been recorded. On the 25th of November 1994 an earthquake of magnitude 4.6 took place with its hypocentre in the geothermal field at 2 km depth; its possible source is related to the northern part of the Los Humeros fault (Lermo, 1999). This earthquake is the main reason for passive seismic studies being conducted at the geothermal field, through monitoring with the existing seismic network. Monitoring stations were set up in December, 1997 and have since been recording continuously.

The M_d magnitude is based on the measured duration (t) of the recorded seismic signal after the arrival of the P wave until the amplitude of the signal is lost in noise. This magnitude is defined by the following relationship:

$$M_d = a + b\log t + c\log t^2 + d\Delta \qquad (1)$$

where t = The recorded seismic duration in seconds;
Δ = The epicentre distance in km; and
a, b, c and d = Constants determined for every station.

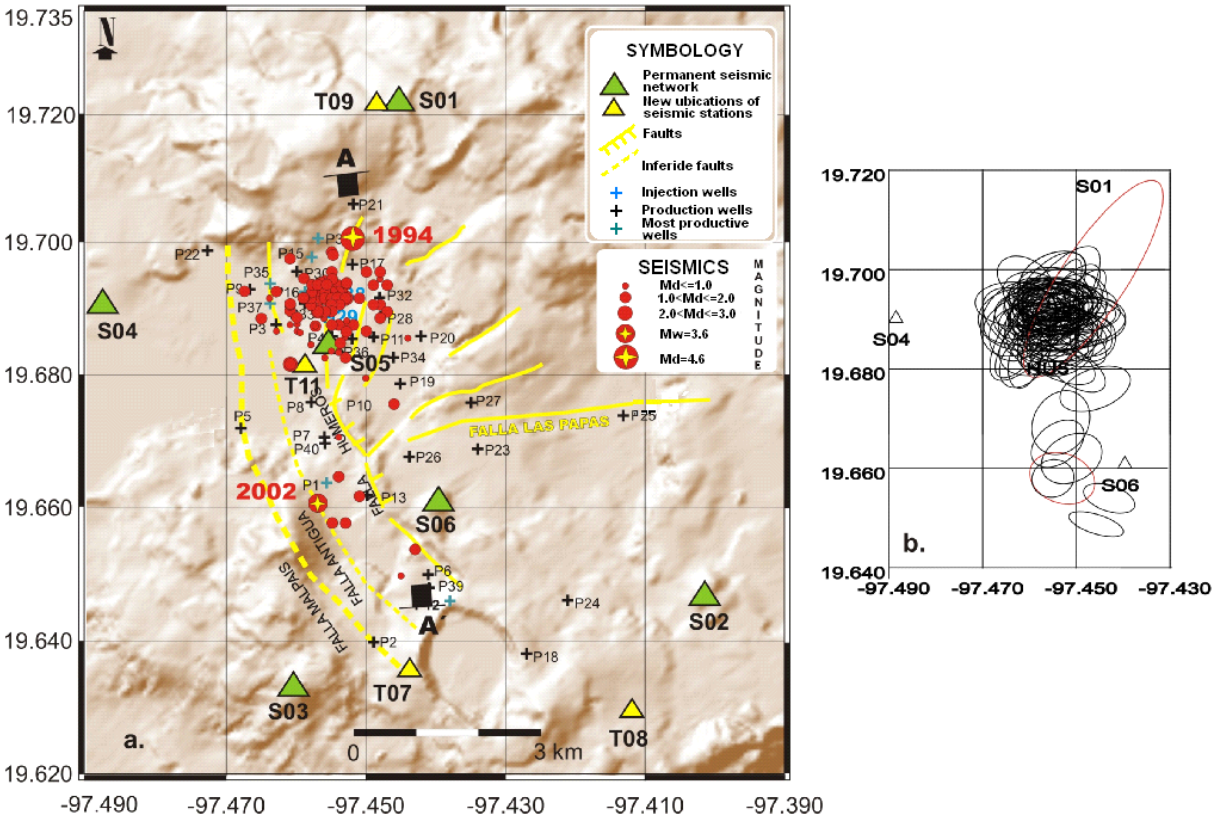

FIGURE 6: a) Epicentric distribution of 95 micro-seismic data events in the Los Humeros field, b) Error ellipses of localization (by Antayhua, 2007)

Generally, the seismic activity is concentrated in the northern zone of the geothermal field, which is the production zone, and in particular in the northwest part where well H-43 is located. Micro-seismic events in the northern part of the Los Humeros fault and a few micro-seismic events in the southern zone originate from the central part of the La Antigua fault (Figure 6). The most important earthquakes are of duration and weight magnitude, M_d = 4.6 and M_w = 3.6, dating from 1994 and 2002. Both are located inside the geothermal field. The error ellipses indicate the accuracy of the epicentre location. The red points in Figure 7a represent the micro-seismic activity from1994 and 2002. The error ellipses from the first period is approximately 2 km in the maximum axis (Lermo, 1999), as presented by the regional seismic networks made available by the National Seismology Service and the Seismic-telemetric System of Information of Mexico (SSN, SISMEX). The black error ellipses (Figure 7b) represent the 95 seismic events that can be seen with less than 1 km in the maximum axis.

The seismic hypocentre distribution has been represented on a stratigraphic profile by Cedillo (1997) and Arellano et al. (2000) with a profile direction N-S (cross-section A-A' in Figure 7). The distribution can be seen to spread between 0.2 km and 4.0 km depth. The shallow seismic events at 0.2-1.0 km are located in layers of pumice, basalts and ignimbrites. An important grouping is observed from 2.0 to 2.5 km depth corresponding in location to the hornblende andesite strata. Another group of micro-seismicity is scattered below that from 2.5 to 4.0 km in the limestone strata. The profile also notes that the 1994 earthquake (4.6 M_d.) originated between impermeable layers and the limestone at 2.0 km depth, whereas that of 2002 (3.6 M_w) was located in the southern zone at 2.3 km depth, between the reservoir and intrusions (Figure 7).

Seismic data was recorded in the time interval from December 2005 to October 2006. The two data sets were analyzed and used to interpret all information of local seismicity in the Los Humeros field, prior to designing and drilling well H-43. The analysis and results of 35 micro-earthquakes of magnitude of durations (M_d) between 0.9 and 1.8, and hypocentre depths ranging from 1 to 4 km, with

the main concentration at 2-4 km, established that well H-43 is located in an active seismic zone. This seismic activity is associated with a system of N-S orienting faults, the La Antigua and La Cuesta faults. These fault zones were encountered in the production wells H-35 and H-37D and the system is considered to be active (Lermo et al., 2006).

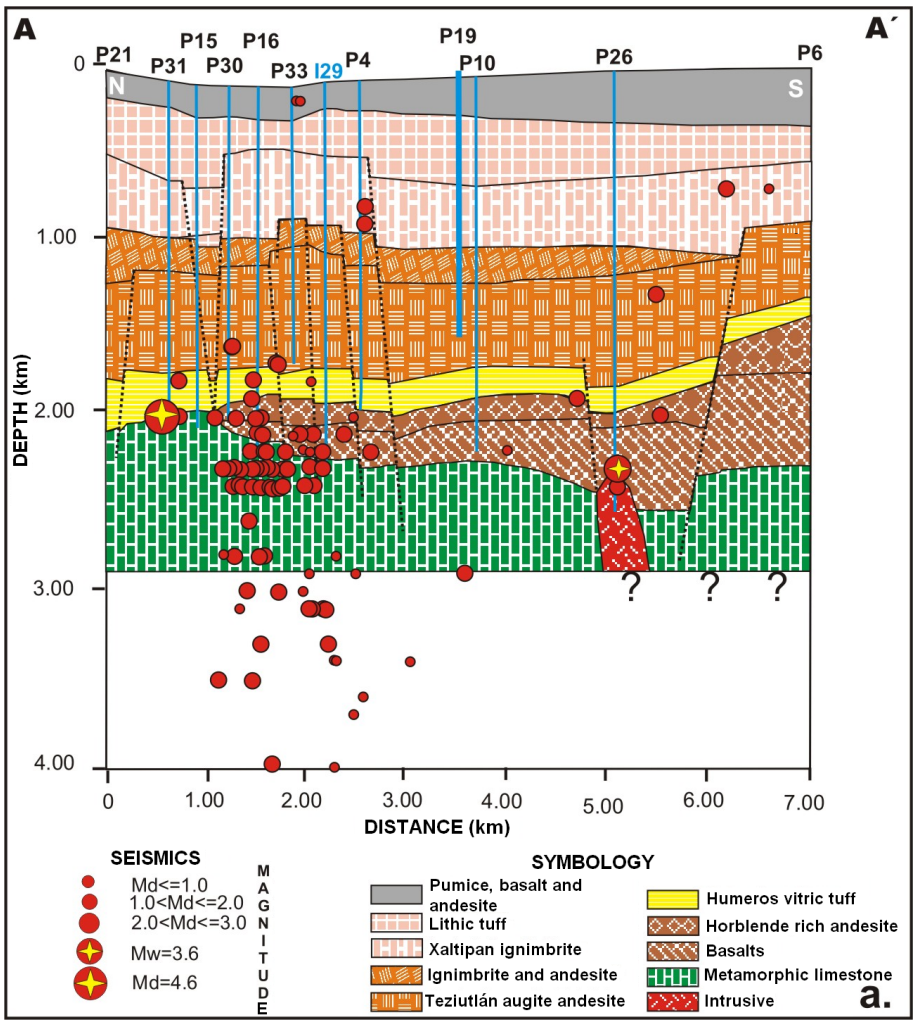

FIGURE 7: Stratigraphic profile of the Los Humeros geothermal field (by Cedillo, 1997 and Arellano et al., 2000), and seismic hypocentre distribution, N-S direction (A-A´), by Antayhua, 2007

The geothermal zone of interest in well H-43 is in the depth range of 1300-2200 m. About 57% of the total micro - earthquake activity in the whole geothermal field takes place in this zone. The most suitable target depth is, however, at 2300 m where 74% of the micro-seismicity in the north zone is concentrated, indicating the possibility of finding more fractures near that depth.

4. DRILLING WELL H-43

The location of well H-43 at the Los Humeros field is shown in Figure 8. It is in the northern zone of the geothermal field, between production wells H-35, H-33, H-9, H-3D, H-16 and south of well H-37D; these production wells were drilled to total depths of 1690, 1600, 2500, 1860, 2048 and 1800 m, respectively.

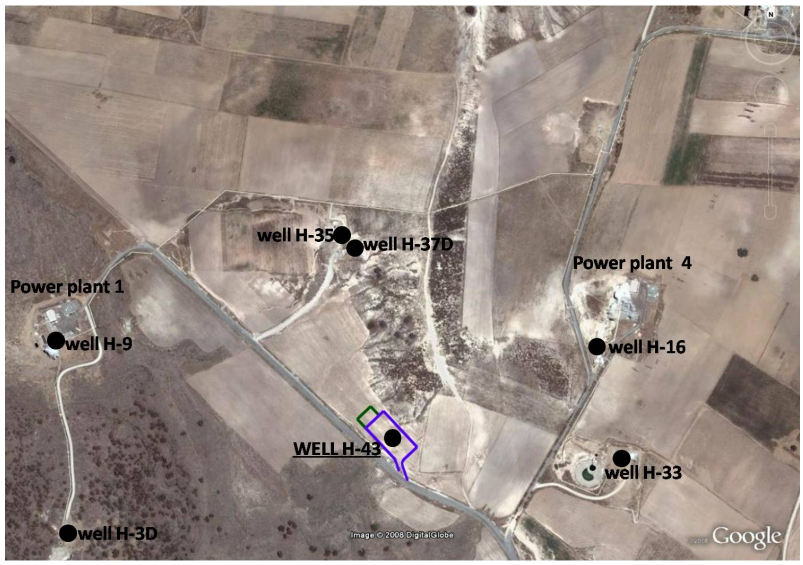

FIGURE 8: Location of well H-43 at the Los Humeros geothermal field

Well H-43 is the first of three new production wells, in

addition to 20 existing production wells. These wells supply steam for the 46 MW Los Humeros II project. Well H-43's geographical coordinates are: X = 661240 m E, Y= 2178060 m N, in reference to the local coordinate system (ITRF 92). The drill site elevation is 2780 m a.s.l.

The design of well H-43 (see Figure 9) is vertical. The Los Humeros geothermal field also has directional production wells, e.g. H-3D and H-37D. The well was spudded on October 22nd 2007 with drill rig IDECO 2, pre-drilling the well with a 40" bit down to 5 m measured depth for the 30" surface casing.. The entire drilling operation required 89 working days. The deeper sections of the well were drilled in 4 stages using a larger sized drill-rig to accommodate this well's wide diameter design. The first stage was drilled with a 26" drill bit down to 52 m for the 20" surface casing, with the casing shoe located at 47.13 m. The second stage was drilled with a 17 ½" drill bit down to 505 m for the 13 ⅜" anchor casing, with the casing shoe located at 501.5 m. The third stage was drilled with a 12 ¼" drill

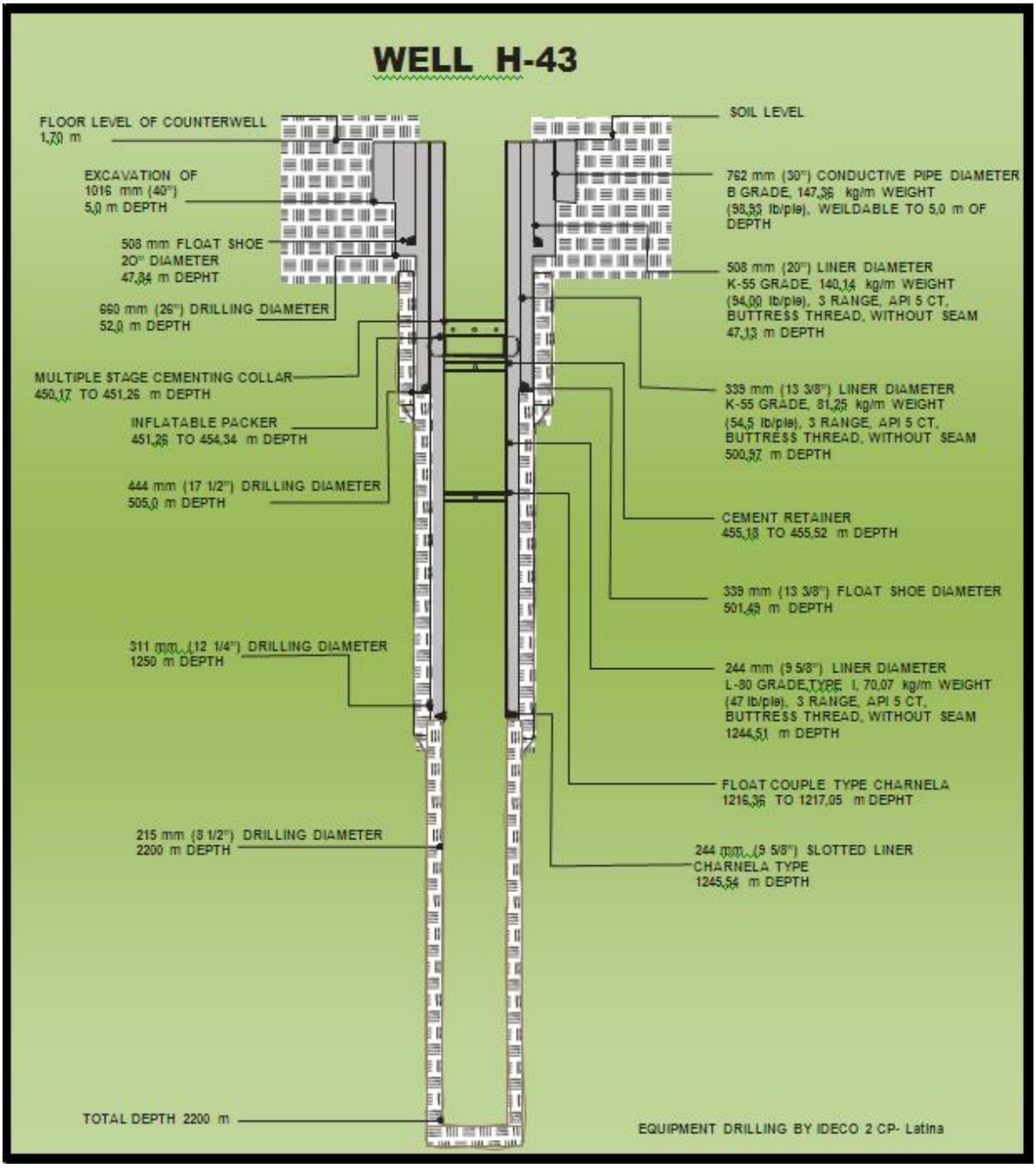

FIGURE 9: Design of well H-43

bit down to 1250 m for the 9 ⅝" production casing, with the casing shoe located at 1245.5 m. The production part of the borehole is open-hole and was drilled with an 8 ½" drill bit down to 2200 m depth. During drilling no problems occurred. Drilling operations were concluded on January 7th 2008.

All drilling operations of well H-43 were conducted by the Mexican drilling company, LATINA, and all the geological and geophysical data acquisition was conducted by the Residencia Los Humeros and Geothermal Projects Management of the Comision Federal de Electricidad (C.F.E.). The well was drilled in 5 stages after the pre-drilling stage was concluded. An overview of all the drilling stages and casing point details are shown in Table 2.

TABLE 2: Drilling and casing depths in well H-43

Drill-Rig	Stage	Depth (m)		Bit size (")	Casing type (")	Section depth (m)	
		From	To			From	To
IDECO 2	Pre-Drilling	1.70	5	40	30	1.70	5
IDECO 2	1. stage	5	52	26	20	5	47.13
IDECO 2	2. stage	52	505	17 ½	13 ⅜	47.13	500.97
IDECO 2	3. stage	505	1250	12 ½	9 ⅝	500.97	1244.51
IDECO 2	4. stage	1250	2200	8 ½	Open-hole	1244.51	2200

5. LITHOLOGY, ALTERATION AND FEED POINTS

Well data for geology and hydrothermal alteration analysis are based on drill cuttings and core samples. The drill cutting samples were collected at 10 m intervals to make interpretations with regard to lithology and alteration minerals, such as quartz, epidote, and chlorite.

5.1 General lithology

The interpreted borehole lithology is based on the macro- and microscopic interpretation of drill-cuttings and cores samples (see Figure 10) from the surface down to 2200 m. The interpretation allowed the determination of four major lithological units in the borehole.

Unit 1. Volcanic deposits of the formation part of the final scoria of the Los Humeros caldera: lithic tuffs, pumice, basalts, andesites and scoria, interpreted as a shallow aquifer (Quaternary).

Unit 2. Pyroclastite deposits associated with the eruptive stage explosions of the caldera; they constitute of big volumes of ignimbrites, characterised by variable gross-thicknesses between 400 and 800 m and are not of geothermal interest.

Unit 3. Volcanic pre-caldera deposits that primarily consist of augite and hornblende rich andesite deposits with, in

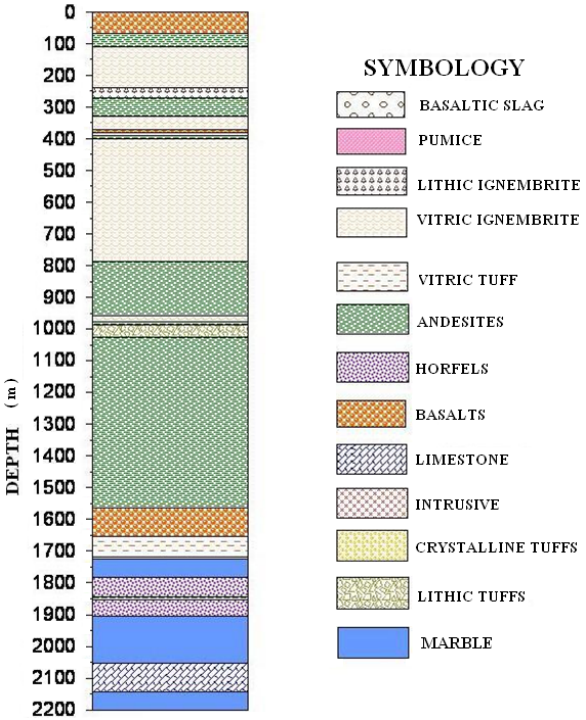

FIGURE 10: Lithological cuttings profile of well H-43

between, alternating basalt and tuff sequences where most of the circulation loss zones were recorded with associated fracture and fault permeability; this is considered the most interesting unit for geothermal production. The unit is interpreted to be of Tertiary age.

Unit 4. The basement of the field is represented by Upper Cretaceous marl and limestone sequences that are affected by re-crystallization due to contact metamorphosis caused by Post-Cretaceous intrusions.

The detailed lithological log presented in Figure 10 is based on the interpretation of cutting samples taken every 10 m. A list of the petrographic descriptions of the cutting samples is shown in Table 3.

5.2 Alteration

An overview of alteration mineral distribution and zonation is presented in Figure 11, which indicates a regular progressive hydrothermal alteration sequence with increasing depth for the well. The secondary mineral zone distribution (Figure 11) shows the calcite zone from the surface down to 785 m within lithic tuff and ignimbrite formations. The chlorite zone exists from 800 down to 1250 m, and the quartz zone of 15-25% of sample content is presented at an interval from 750 to about 1000 m

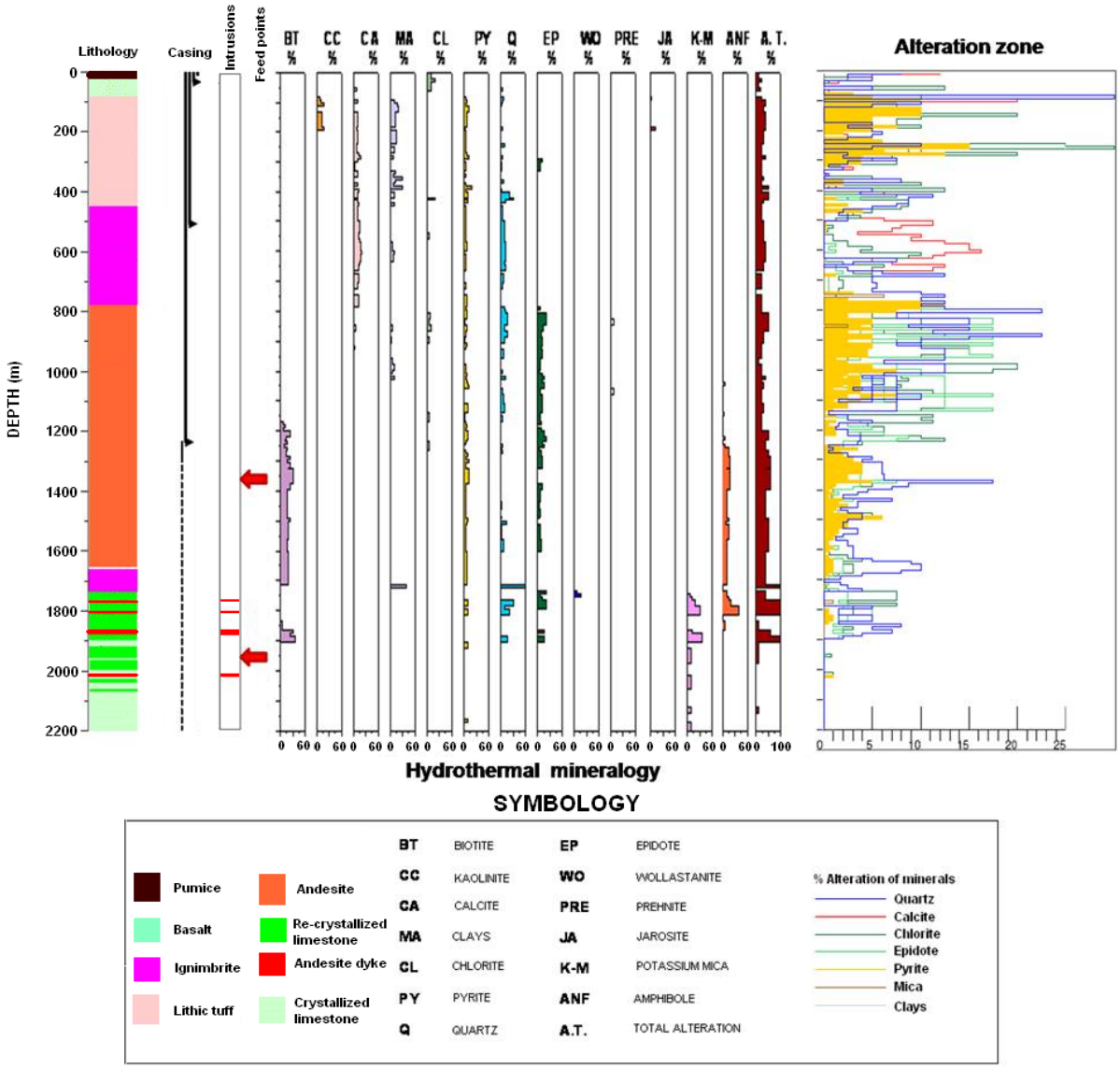

FIGURE 11: Hydrothermal mineralogy and alteration zone distribution of well H-43

depth. Quartz occurred during drilling from a depth of 1895 m. Pyrite was seen in all sequences in its finely distributed form, except between 800 and 1265 m, where the pyrite content increased to 7%, mainly as a part of micro-fracture fillings.

According to Viggiano and Robles (Viggiano and Flores, 2008), their para-genesis zoning proposal suggests the existence of areas related to high temperatures (above 200°C), represented by the association of mineralogical Ep + Qz+ Cl sequences, first found at a depth of 785 m. The high total rock percentage (25-50%) of alteration minerals in the andesitic formation, and the existence of areas of circulation losses (after cleaning and thermal breakthrough of well H-43) lead to the conclusion of movement of geothermal fluid between 785 and 1265 m.

5.2.1 Fluid analysis and chemistry

Drilling mud samples were collected every 25 m from 500 m downwards, and the gas content was sampled every 25 m, with the purpose of determining the mud input and output parameters of pH, electrical conductivity, and the contents of arsenic, boron and sulphate. The emanations from gas bubbles were led into a flask containing 75 ml of NaOH 4N to determine the contents of H_2S and CO_2. The results of these parameters (Figure 12) are useful for identifying areas of interest which show

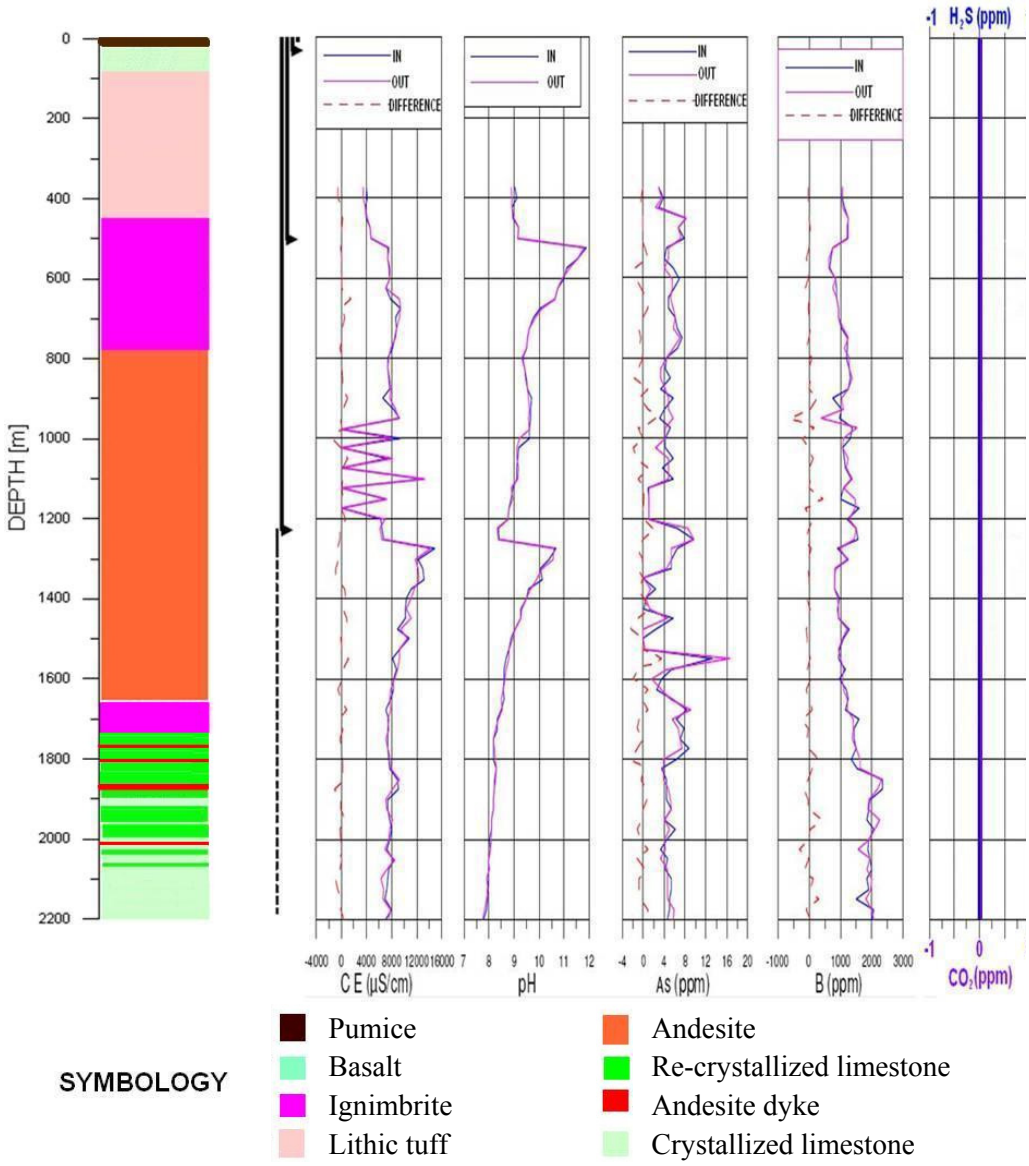

FIGURE 12: Chemical parameters during drilling of well H-43

increased geothermal activity; these should be correlated with the geological and temperature logging information to make a better interpretation of the main feed zones in the well. However, looking at the drilling mud analysis, as shown in Figure 12, the logged drilling mud chemical parameters indicated no significant changes that might be related to areas of interest. Also, in the gas samples no H_2S or CO_2 was observed.

The results of the physical-chemical sampling made during drilling did not help to identify input areas of the well. One could also keep in mind that the cause for no gas observations could lie in the characteristics of the drilling mud, i.e. the mud-cake sealed off the borehole while drilling and made it difficult for reservoir fluids to enter the borehole.

5.2.2 Petrographic analysis and zonations

During drilling, 206 cutting samples were obtained for petrographic analysis and interpretation. This included primarily the zone distribution of hydrothermal minerals for well H-43(see Table 3), along with their genetic implications and a comparison with hydrothermal areas that had been originally proposed. Table 3 gives an overview of the alteration zones, showing the first alteration zone referred to as acid sulphate / bicarbonate. The sulphate acid minerals include: kaolinite, pyrite, anhydrite, jarosite and chalcedony and the bicarbonates are mostly calcite and smectite / chlorite.

TABLE 3: Hydrothermal-mineralogical zoning, depth, associated and in situ alteration minerals and reservoir observations of well H-43, Los Humeros geothermal field (Viggiano and Flores, 2008)

Alteration zone	Depth (m)	Mineralogy	Remarks
Acid-sulphate alteration, carbonated; Zeolite zone	0-290	Clorite/smectite+calcite+zeolites (bicarbonate). Kaolin group+pyrite+ anhydrite+ jarosite+chalcedony+ (sulphatara acid)	Alteration of vadose zone, due to a mixture of sulphate acid fluids and bicarbonate. Deuterium alteration, maybe also meteoric (100-200°C).
Incipient epidote-calcite; Epidote zone	290-785	Calcite+quarz+pyrite+/- montmorillonite+/-illite+/-incipient epidote	Direct alteration (boiling) and replacement below level of chloride sodium fluid (>220-250°C).
Epidote; Epidote zone	785-1145	Epidote+quarz+chlorite (peninite) +/-prehnite	Same as above (>250-<350°C)
Amphibole-biotite; Amphibole zone	1145-2200	Epidote+amphibole+biotite+pyrite+/- quarz+pyrite+/-peninite+/-white mica (after to 1755 m)	Same as above (>350°C)

The sulphate acid minerals were formed by the incorporation of gas such as H_2S into meteoric fluids from surface aquifers, and the bicarbonate minerals were formed by re-incorporation of gas such as CO_2 into the same meteoric fluids. The sulphate acid and bicarbonate minerals would be diluted or ionized and ready to react in the vadose zone, i.e. above the phreatic level. This observation is in contrast with the assumption that the main sources of H_2S gases exit preferably in the up-flow and that CO_2 gases exit into the marginal parts of the geothermal system, i.e. in the out-flow.

It is known that both processes can occur, the escape and re-incorporation of both gases, during natural boiling of the system. This is implied by the existence of zeolite minerals that were found in this zone that do not correspond with any of the known mechanisms for this formation, unless a neutralized phase of acid-sulphate fluid existed which could explain the formation of these zeolites by the deuteron process, i.e. a secondary reaction with the basaltic rock formation that occurred later (Viggiano and Flores, 2008).

5.3 Intrusions

Intrusive rocks have been recorded through the macro- and microscopic interpretation of drill-cuttings and core samples; that interpretation allowed the determination of lithological unit 4 (see Section 5.1). As a result, intrusive rock intensity can be described as increasing with depth, see Table 4. In well H-43, Jimenez Salgado estimated the intrusive rock intensity for each successive 10 m depth interval in the well. The results of his review suggest that the re-crystallized limestone sequences primarily consist of light to dark grey coloured cuttings between 1725 and 2200 m, and are very likely cut by four andesitic dykes. The re-crystallization of the limestone is due to the presence of metamorphism, documented by alteration indications of the limestone.

TABLE 4: Intrusive rock intervals in well H-43

Type	Depth interval (m)
Andesitic dykes	1770-1775
	1805-1810
	1865-1875
	2015-2020

A considerable part of the intrusive dykes are composed of intermediate andesites, judging from the increased abundance of re-crystallized limestone into marble with increasing depth, and appear to become more acidic with increasing depth. With an equilibrium diagram between phases, and empirical observations, it is possible to predict a pH less than 5. The mineral calcite is also an indicator of acidity, e.g. in well H-43, calcite was observed at 60 m depth and disappeared totally at 785 m depth. The calcite has pH restrictions during formation with temperatures around 300°C and can only form in conditions of pH>5. This could explain the decrease or total disappearance of calcite at pH values between 2 and 3, with increasing depth and temperature in the well. Figure 13 shows a good comparison between cutting descriptions and logging data with regard to an identified intrusion.

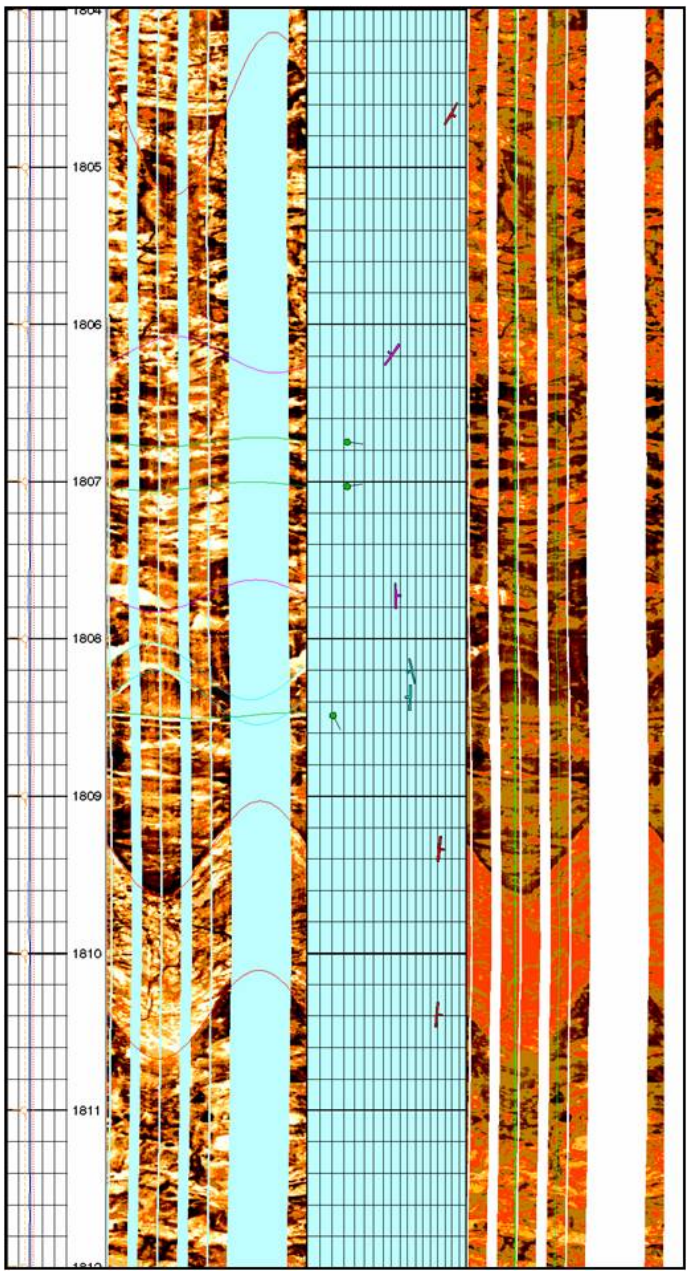

FIGURE 13: FMI image of interval 1804-1812 m showing a good comparison between cutting descriptions and logging data with regard to an identified intrusion at 1810 m

5.4 Feed points

Circulation losses were monitored during the entire drilling operation. A total circulation loss was recorded between 50 and 70 m (see Figure 14), located within a series of basaltic lava flows, that could possibly have been due to the influence of the La Cuesta fault. Other than that, the well did not show any further circulation losses that could be linked to feed zones during drilling. A possible reason for this tight well behaviour could also lie with the heavy mud weight used; during drilling, the mud-cake closed up feed zones which later opened up during hole cleaning by water injection (see Section 6.1.1), the final well test, and the well's thermal breakthrough. The list of feed zones obtained from the temperature and pressure analysis will be referred to in Section 6.1.3.

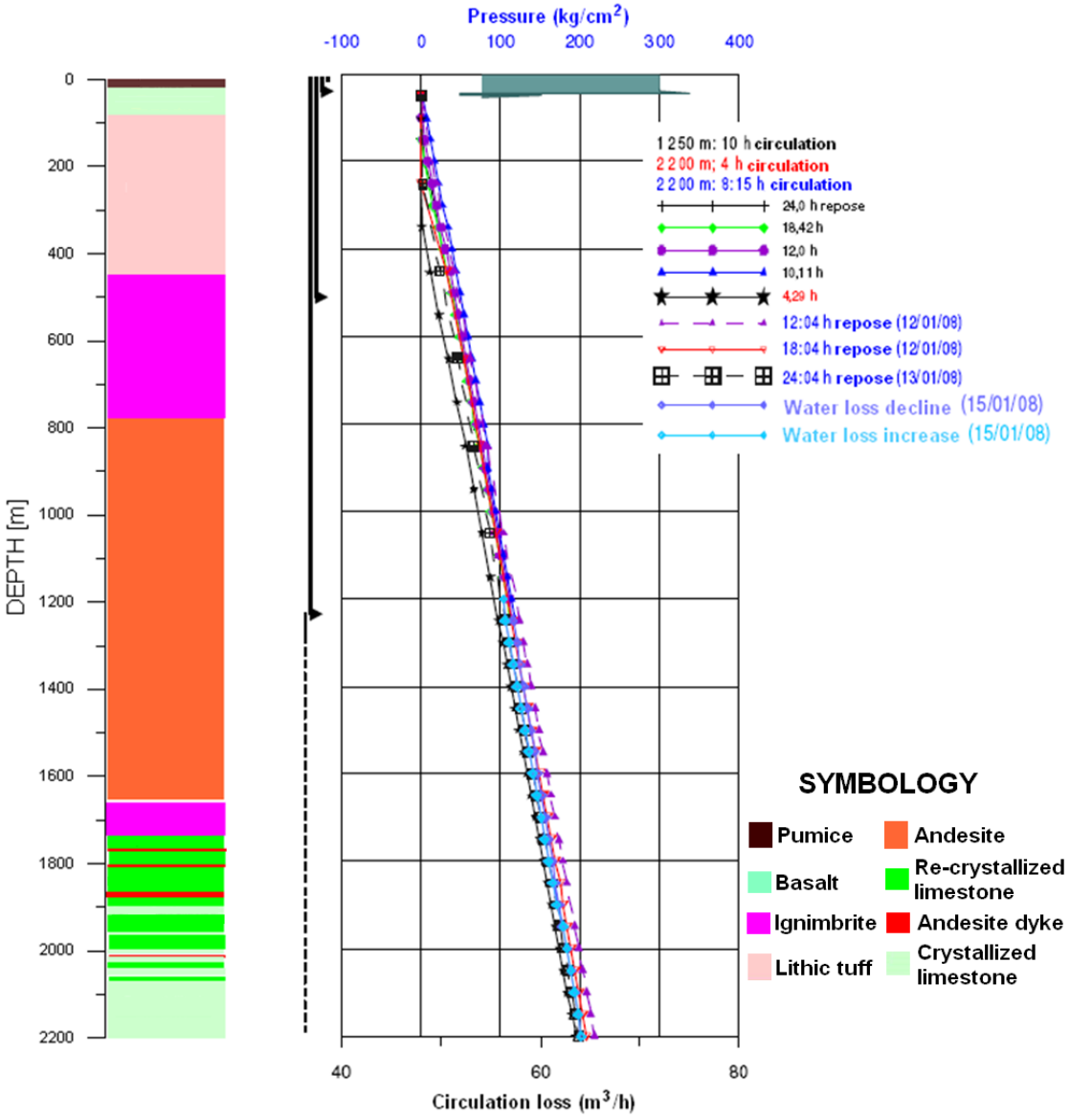

FIGURE 14: Circulation loss measurements during drilling of well H-43

6. BOREHOLE LOGGING AND ANALYSIS

Borehole geophysical parameters were recorded and analysed using Petrophysical analysis (1245-1626 m); Compound open hole logs (1245-1630 m); SonFrac fractures estimation (1245-1620 m); Dipole

Shear Sonic Imager (1245-1626 m); ROXAN stability estimation (1245-1630 m); Fullbore Formation MicroImager (FMI) fractures analysis (1250-1634 m); FMI fracture analysis (1711-1813 m) and FMI Stereonet&StrucView (1711-1811 m). Table 5 summarises the use of geophysical measurements recorded in well H-43. The maximum temperature recorded with temperature logs was 325°C. The subsurface lithology was identified by inspection of drill cuttings every 10 m. In the depth range of 0-1735 m, a heterogeneous alternation of volcanic deposits was found; in the depth range from 1740 to 2200 m, a sedimentary calcareous sequence was found, affected by andesitic dykes, metasomatic processes, and hydrothermal activity of high temperature within the marble formation.

TABLE 5: Geophysical measurements recorded in well H-43, acquired using a single instrument provided by Schlumberger (S/N 3096)

Date	Logging company	Depth (m)	Objective	Logging campaigns
09.01.2008	Schlumberger	1245-1626	Caliper; Geological log Lithology; Formation evaluation; Collapse	*Petrophysical analysis* Circulation stopped 11:00 Logger on bottom 16:25 Max. rec. temp.: 180°C Type of fluid in hole: Bentonite
09.01.2008	Schlumberger	1245-1630	Closed cave; Collapse; Geological log; Drilling; Caliper; Lithology; Porosity	*Compound open hole* Including records with environmental corrections
09.01.2008	Schlumberger	1245-1620	Closed cave; Collapse Caliper; Drilling; Estimate locations of fractures and permeability of formation; Porosity	*SonFrac fractures estimation* STRC UP; STRC Down; FWiD BHT: 180°C Bitsize: 8.5”
09.01.2008	Schlumberger	1245-1630	Casing; Cave; Formation evaluation; Drilling; Caliper; Elastic constant; Pressure; Compressibility; Elastic constant; Stress; Strain	*ROXAN stability estimation* Elastic model calculation utilized with unique component model for isotropic and heterogeneous environment. Resistance of rocks calculated with correlation of Coates-Denoo. Friction angle was obtained using Plumb correlation. Horizontal efforts calculated using pore-elastic model. Pore pressure gradient used 0.45 psi/ft (fixed value used in the model).
09.01.2008	Schlumberger	1626-1245	Collapse; Compressibility Shear; Porosity Geological log; Drilling; Caliper; Formation evaluation P-wave to travel; S-wave to travel; Fractures	*Dipole shear sonic imager* Circulation stopped 11:00; Logger on bottom 16:25; Max. rec. temp.: 180°C; Type of fluid in hole: Bentonite
10.01.2008	Schlumberger	1250-1633	Drilling; Casing; Borehole; Mud; Geological log; Geological fault; Porosity	Fullbore Formation MicroImager fracture analysis
10.01.2008	Schlumberger	1711-1813	Drilling; Casing Borehole; Mud; Geological log; Porosity; Geological fault	Fullbore Formation MicroImager fracture analysis

6.1 Temperature and pressure logging

Temperature data obtained in wells serve as critical input to fields of geothermal exploration. The temperature logs can detect thermal anomalies between the well fluid and the formation fluid. More information can be obtained from the identification and interpretation of these anomalies (Doveton

and Prensky, 1992). Analysis of well temperature data is the main step required for quantitative assessment of geothermal reservoirs (Lashin, 2005).

Estimation of formation temperature depends on the conditions of a well. The presence of flow in a well screens the conditions in the formation and makes the determination of the formation temperature less straightforward. In well H-43 two temperature and pressure surveys were performed, one at 1250 m, after drilling the 12 ¼" diameter well section, and the second survey to the total depth of 2200 m, after drilling the final 8 ½" diameter well section.

The first temperature survey at 1250 m was performed using a mechanical instrument (Kuster), obtaining temperature logs taken 6, 12, 18 and 24 hours after drilling ended. These logs were needed to calculate the stabilized temperature. The temperature logs were recorded in open-hole, and obtained four profiles of temperature and pressure taken at the times mentioned above. In this depth range, no circulation loss was visible (see Figure 15). The water table taken after 6 hours was located at a depth of 41 m, and after 24 hours it had decreased to 150 m depth, indicating that the well was accepting fluid. The temperature profiles show one permeable zone, *between 1000 and 1200 m depth.*

The most common method used to estimate static formation temperatures is the *Horner method* or *Horner plot:*

$$T_{ws} = T_i - m \log\left(\frac{t_c + \Delta t}{\Delta t}\right) \tag{2}$$

where T_{ws} = Well shut in temperature (°C)
T_i = Initial temperature (°C);
m = Slope;
Δt = Gradient time.

We obtain a straight line with slope:

$$m = \frac{2{,}303Q}{4\pi T} \tag{3}$$

where Q = Production;
T = Transmissivity.

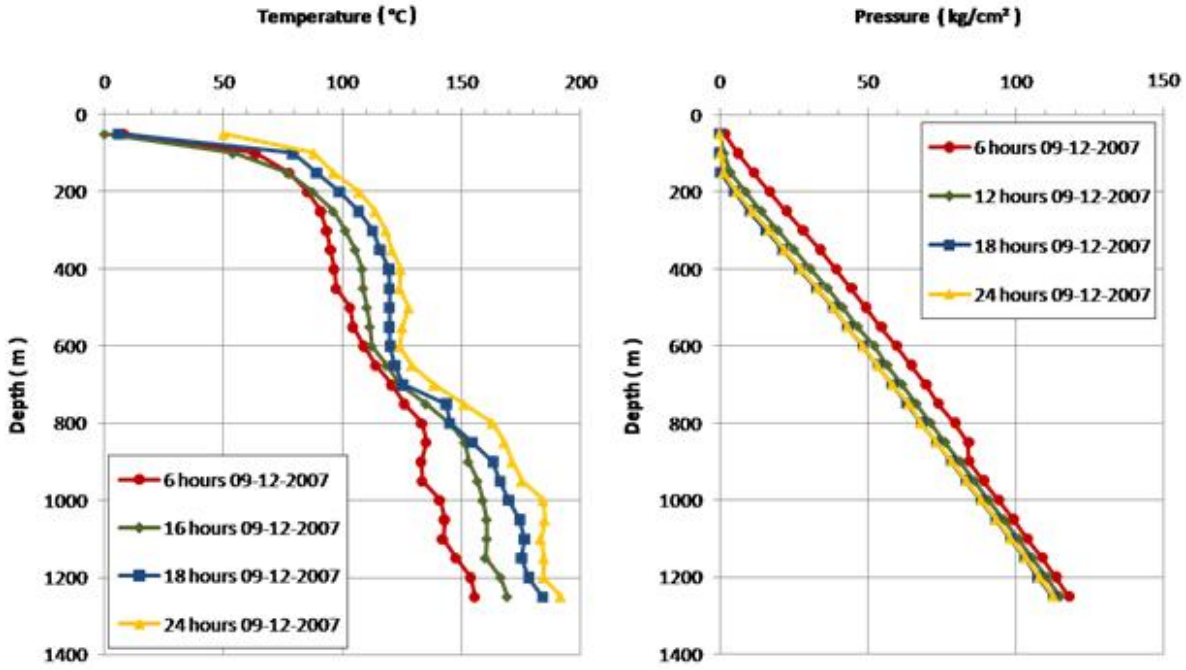

FIGURE 15: Temperature and pressure profiles of well H-43 to 1250 m depth

This model describes a straight line of slope *m,* and the intercept T_i is the static formation temperature (SFT), which is obtained by extrapolation to infinite shut-in time. However, we cannot wait that long, so we extrapolate the line to:

$$\frac{t_c + \Delta t}{\Delta t} = 1 \tag{4}$$

The Horner method has been widely used in the geothermal industry, although it underestimates static formation temperatures (Ascencio et al., 1994). Practical considerations require that these temperatures be measured at the bottom of the borehole where circulation times are on the order of a few hours so that the straight line is clearly defined (Dowdle and Cobb, 1975). The temperature logs were used to calculate the stabilized formation temperature of 228°C at 1250 m depth, see Table 6 and Figure 16.

TABLE 6: Stabilized temperature calculated at 1250 m depth by Horner plot (Sánchez and Torres, 2008)

Drilling time 1247-1250 m = 0.75 h		**Circulation time = 10 h**	
Profile number	**After time (hours)**	**Temperature (°C)**	**Horner time (no dimension)**
T1	6	155.6	0.298
T2	12	169.35	0.263
T3	18	184.17	0.188
T4	24	191.74	0.151

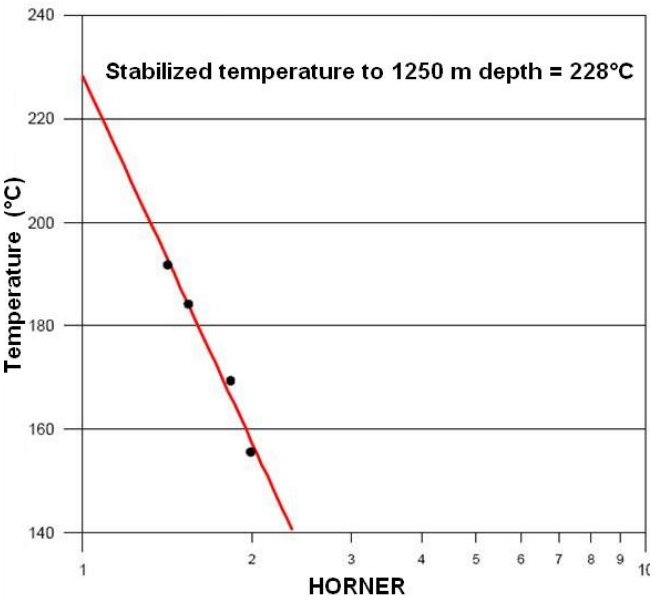

FIGURE 16: Semi-log graph for stabilized temperature calculation to 1250 m depth in well H-43 (Sánchez and Torres, 2008)

During drilling of the 8½" diameter well section (prior to the second survey), no circulation loss of drilling fluid was detected. The reservoir has low permeability above the major feed zone and, as mentioned before, it is possible that the drilling fluid screens the permeable zones. Only the logs were capable of identifying the possible feed zones; they also evaluated the thermal properties in the open-hole section of the well.

The second survey recorded four pressure and temperature logs in the open-hole section that were taken 6, 12, 18 and 24 hours after the end of drilling (see Figure 17).

The pressure logs show water table change from 50 m depth after 12 hours to 250 m depth after 24 hours. By using the well's geometry (internal diameter = 0.2204 m) together with the water table drop of 200 m in 12 hours, it can be calculated, assuming linear water table drop in time, that the formation was accepting 0.63 ton/hour during the recording of the logs, indicating that the formation has low permeability, even if the temperature profiles may not reliably identify the feed zone interval.

The stabilized temperature at 2200 m depth is 383°C (Table 7 and Figure 18), which is above the critical point of water (374.15°C). The pressure is, however, not high enough to achieve the supercritical point (above 22 MPa). Note that the pressure curves do not correspond to the temperature profiles for pure water, in accordance with the existence of mud in the well.

TABLE 7: Stabilized temperature calculated at 2200 m depth by Horner plot (Sánchez and Torres, 2008)

Drilling time 2197-2200 m = 0.75 h		**Circulation time = 8.15 h**	
Profile number	**After time (hours)**	**Temperature (°C)**	**Horner time (no dimension)**
T2	6	272.04	2.48
T3	12	287.63	1.74
T4	18	310.85	1.49
T5	24	330.33	1.37

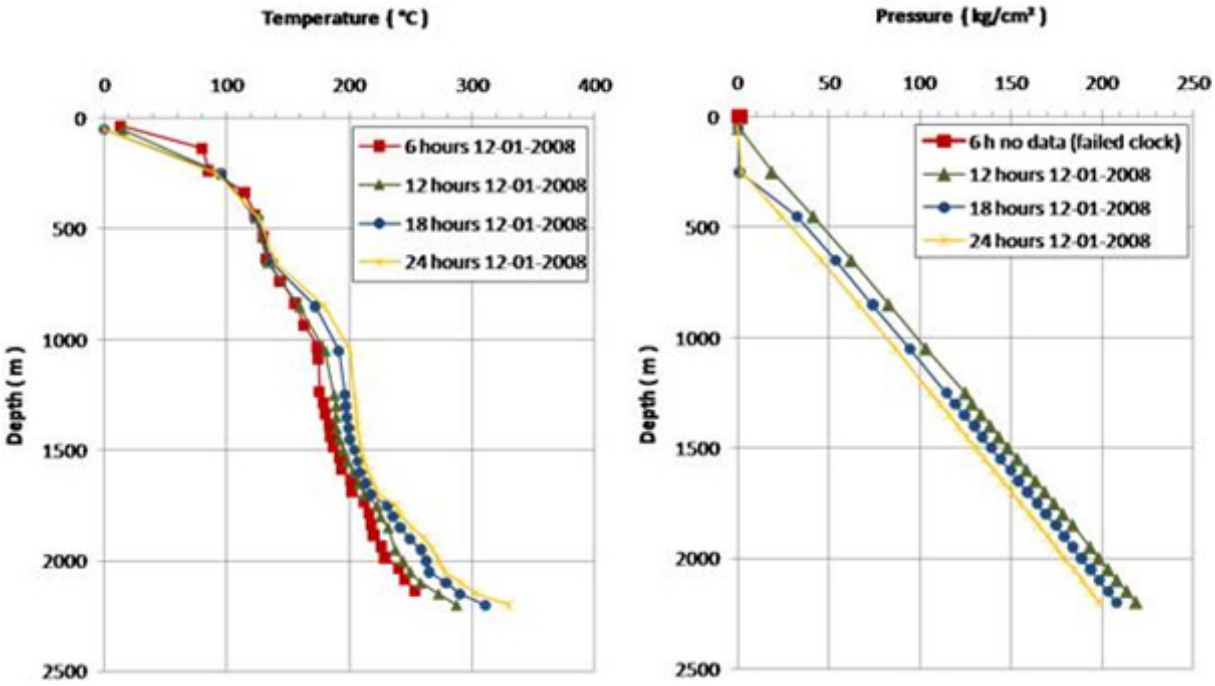

FIGURE 17: Temperature and pressure profiles of well H-43 to 2200 m

6.1.1 Water loss test

The well did not have circulation losses, because the mud-cake was grouting the possible feed points. Therefore, it was necessary to inject water into the well for cleaning, in two stages:

Stage 1: Injection of geothermal water was performed in steps through the drill string, until it reached the bottom of the well. During this activity, a partial fluid circulation of 60 m^3/h was achieved.

Stage 2: At depth to 1224.7 m, injection of 150 m^3 of a lignite-water solution with a concentration of 1.0 kg/0.159 m^3 was performed as follows:

- Injection 60 m^3/h for 30 minutes without head pressure applied;
- Increasing the flow rate to 75 m^3/h, reaching a maximum head pressure of 24.6 kg/cm^2;
- Increasing the flow rate again to 90 m^3/h, recording a maximum head pressure of 36.9 kg/cm^2.

The final cleaning of the well, after the water loss test, was carried out in three steps:

Step1: Drill pipe of diameter 4 ½" and length 22.48 m was inserted and connected to a lubricator to support logging instruments.

Step 2: Injection of 60 m^3/h of water through the annular volume for 1.5 hours. An instrument with the two sensing elements for temperature and pressure was used to record to 1250 m depth, at 50 m intervals.

Step 3: Upon reaching the total depth of the well, an upward log was performed. The measurement points downstream and upstream were the same. The water flow rate injected into the well was constant during all tests. The header pressure was recorded giving atmospheric pressure reading. After the end of the test, water injection of 90 m^3/h was continued for 20 minutes, without observing readings of increased head pressure.

Figure 19 shows the pressure and temperature profiles during the test. They identify two points of water acceptance:

- At 1400 m depth, and
- At 1850 m depth.

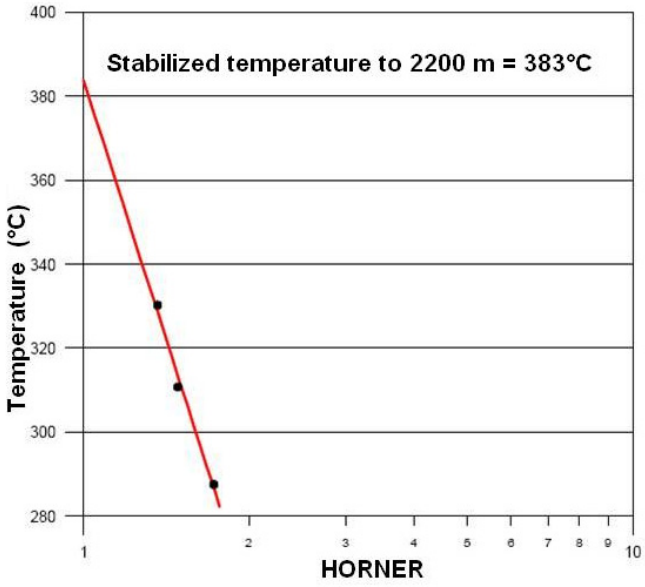

FIGURE 18: Semi-log graph for stabilized temperature calculation to 2200 m depth (Sánchez and Torres, 2008)

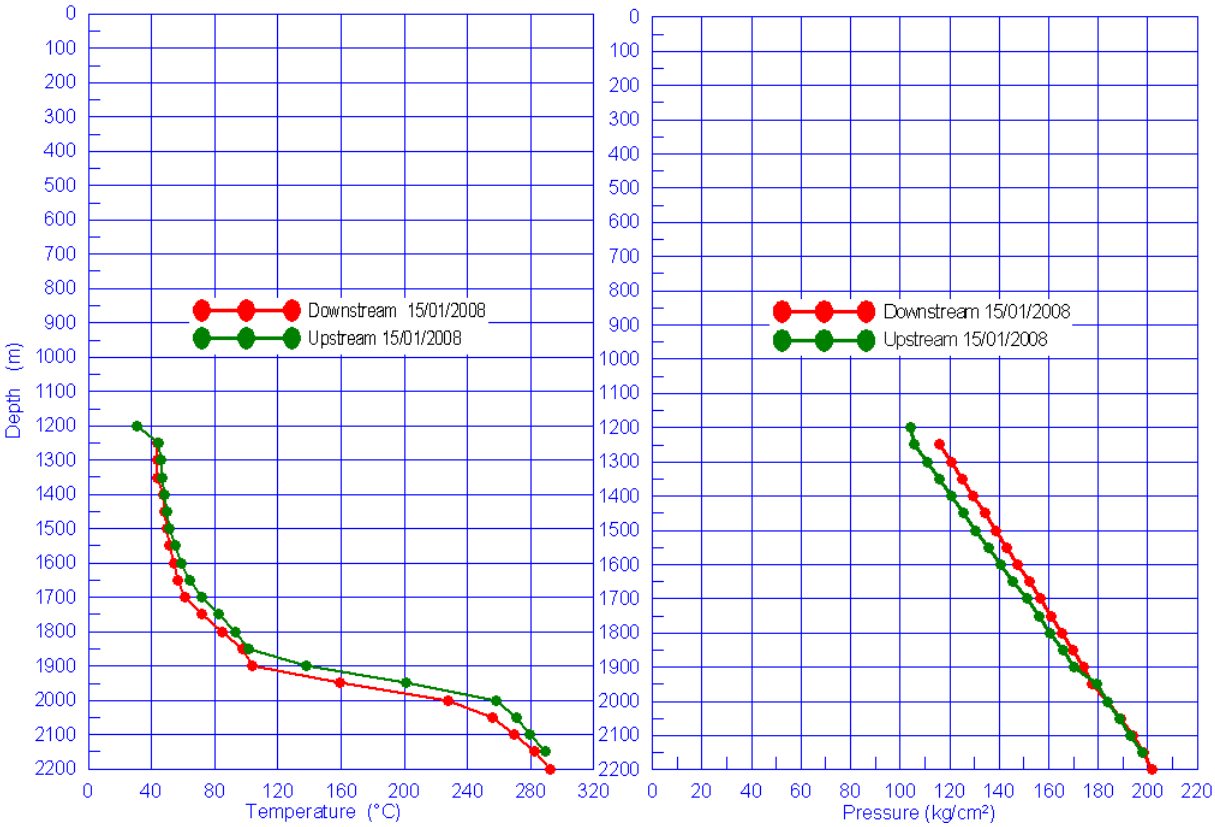

FIGURE 19: Temperature and pressure profiles during the water loss test

6.1.2 Thermal breakthrough

Thermal breakthrough of the matrix rock was performed in three injection-recovery tests, injecting at three different flow rates in each test. The instrument with pressure and temperature sensors was stopped at 1250 m depth. Figure 20 shows the bottom pressure during the test. The development of the test is described below:

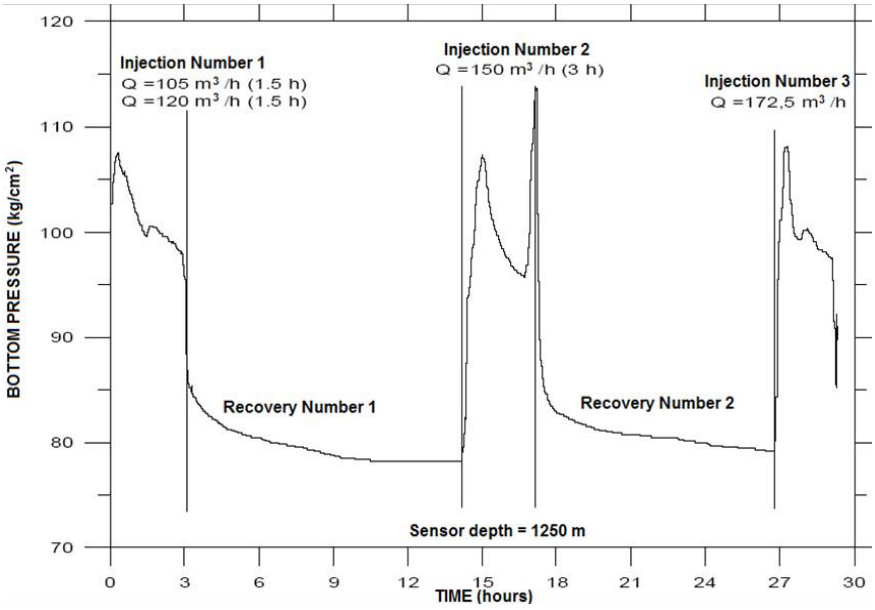

FIGURE 20: Thermal breakthrough of matrix rock (Sánchez and Torres, 2008)

Injection 1. The injection started with 105 m^3/h flow rate (Q) for 1.5 hours, after which it was increased to 120 m^3/h (Q) for another 1.5 hours to complete 3 hours of injection. No head pressure formed during this stage. Recovery stage 1 lasted 11.25 hours. At the injection of 105 m^3/h (Q), the bottom pressure increased to 107.4 kg/cm^2 during the first 10 minutes, and then declined to 99.4 kg/cm^2. During the 120 m^3/h injection, the pressure increased to 100.4 kg/cm^2 for 10 minutes and then declined to 97.9 kg/cm^2 after 1.5 hours. At the end of recovery stage 1, the pressure had declined to 78.4 kg/cm^2.

Injection 2: The injection started with 150 m^3/h flow rate (Q) for 3 hours, with no increase in header pressure. The maximum downhole pressure during injection was 107.2 kg/cm^2, and after that declined to 95.8 kg/cm^2, before finally increasing to 111.7 kg/cm^2 for 5 minutes (the flow rate was constant during the test). It was concluded that there was a light clogging of permeable zones. Recovery stage 2 lasted 8 hours, with a pressure decline to 79.4 kg/cm^2.

Injection 3: The final injection used 172.5 m^3/h flow rate (Q), with no head pressure. The maximum downhole pressure was 108.4 kg/cm^2. The same pressure behaviour was observed as in previous injection tests: the pressure declined after 10 minutes of injection. Recovery stage 3 lasted 10 hours, but no records exist from that interval because the sensor failed.

Figure 20 shows that the downhole pressure during the 3 injection stages increased to a maximum in the first 10 minutes after starting the injection tests, and declined after that. The fluid pressure reached the opening pressure of fractures, causing improvement in the secondary permeability, due to fracturing of the matrix rock. The diagnostic log-log using the pressure and pressure derivative, identified pseudo-radial flow (m = 0′), between 0.8 and 1.35 hours. A Horner semi-log using data corresponding to pseudo-radial geometry, obtained the parameters *kh, S* and *P** (explained below) calculated for injections 1 and 2:

$$kh = 3558.9 \text{ md-m} \qquad S = 3.9 \qquad P^* = 80.05 \text{ kg/cm}^2$$

Using the curve type technique, the pressure data and derivative conform to the curve type of Bourdet (model of homogeneous radial flow acting infinitely). The calculated parameters kh and S for

injections 1 and 2 are:

kh = 3774.75 md-m S = 4.55

The values obtained by both techniques are similar, indicating good reliability in the results. The formation conductivity (kh) is higher than the average value (486 md-m) of the other wells closest to this well. The skin factor (S) is positive (S>0, damaged well or thermal breakthrough) indicating skin in the formation, most certainly by the presence of drilling mud and drill cuttings.

6.1.3 Pressure and temperature logs after the thermal breakthrough test

After the thermal breakthrough tests were realized, pressure and temperature logs were performed, with the purpose of confirming the convective intervals. Figure 21 shows the profiles for this purpose. The medium pressure of the reservoir at 1725 m depth was 120 kg/cm^2. The water table was located at 450 m depth, two main convective intervals were identified, and two feed zones:

- First convective interval was between 1550 and 1900 m depth;
- Second convective interval was between 2050 and 2200 m depth;
- First feed zone interval was between 1250 and 1550 m depth; and
- Second feed zone interval was between 1950 and 2200 m depth.

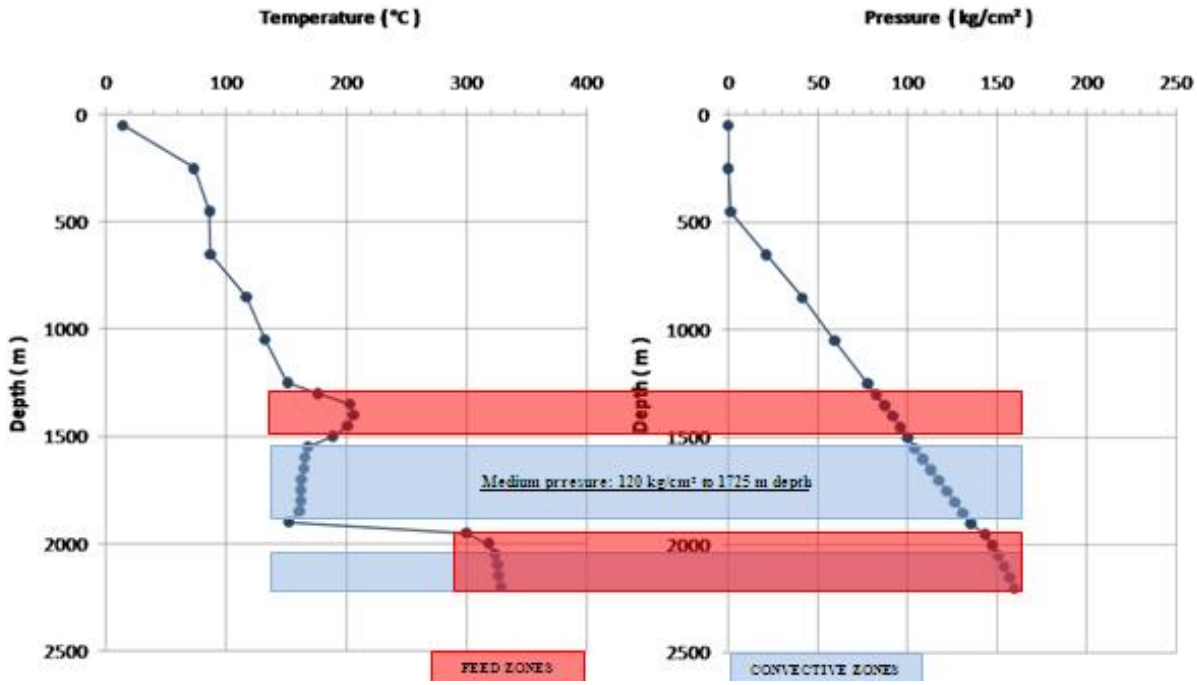

FIGURE 21: Temperature and pressure profile after thermal breakthrough of well H-43

When the pressure profile is compared with the pressure profile obtained after 24 hours, and before the breakthrough tests (Figure 17), it can be seen that the water level dropped from 250 to 450 m depth, indicating flow loss to the formation. In addition, before thermal breakthrough the measured temperature and pressure smoothly increased with depth. After thermal breakthrough, the temperature profile clearly indicated the feed zone interval depths, and permeability improved in the well by the thermal breakthrough process.

6.2 Lithological and acoustic borehole logging

In this section, a brief description is given of the lithological logs, such as natural gamma ray, gamma-gamma, density, neutron-neutron, porosity, and resistivity logs. A log is defined as "a record of sequential data" (Webster). In geophysics this word is mainly connected with continuous measurements carried out in boreholes. In general, logs are valuable for two reasons. The first is to give information on well performance and design. This information is often needed during drilling when logs can play a role in deciding means of avoiding specific problems and in estimating success. Secondly, and even more importantly, logs give information on structure, physical properties and performance of the geothermal system penetrated by the well (Stefánsson and Steingrímsson, 1990).

At the Los Humeros geothermal field, work to satisfy the electrical energy demand is currently ongoing, leading to the identification of new sites for drilling additional production wells. Well H-43 was drilled with this objective in a proposed area of interest which is sustained by structural geology (surface recognition) and where many geophysical studies have been conducted.

Within the area of interest, it was proposed that a new well could intercept the N-S fracturing-faulting geothermal system of the Malpais and Antigua faults that incline due east. Well H-43 pre-drill predictions showed an intersection of the fault zone at around 1300 m depth, and a prediction to reach the top of the limestone at 1800 m well depth, based on obtained information of the top of the limestone from wells nearby (Table 8).

TABLE 8: Top of limestone depth in production wells near well H-43

Wells	Depth (m)	Top of limestone (m)
H-3D	1860	1620
H-9	2500	1720
H-16	2048	2020
H-33	1600	N/A
H-35	1690	N/A
H-37D	1800	1790

The Exploration Department (C.F.E.) suggested carrying out lithological log measurements in the depth interval of 1245-1620 m and the Fullbore Formation MicroImager log (FMI) to the well bottom. Both logs were performed by Schlumberger during drilling. However, the FMI logging was only carried out at two depth intervals, the first between 1250 and 1633 m, and the second between 1711 and 1813 m. Deeper measurements were not possible, due to high temperature recorded in the well (328.6°C was recorded during the thermal breakthrough test on January 15th and 16th 2008).

The lithological logs were acquired by Schlumberger on the 9th of January, 2008. Due to the high temperature in the deeper part of the well, logging needed to be aborted so as not to damage the instruments and did not reach the final depth of 2200 m. The logs were recorded upward with the first point recorded at 1620 m depth and the last at 1245 m depth.

The petrophysical evaluation showed that the gamma ray (GR) log could be used to observe the differentiation of the main lithological intervals (Figure 22). The interval between 1275 and 1292 m corresponds well with a change in lithology with an igneous rock contact, a possible andesitic rock intrusion (observed in drill-cuttings). The interval between 1303 and 1314 m also matched a change in lithology at an intrusion. The interval between 1400 and 1429 m in the GR log gives higher values corresponding to a more acidic lithology (igneous rock) and corresponding to that depth, temperature was measured at 206.1°C. At the intervals of 1474-1480, 1484-1499, 1501-1506, and 1507-1512 m, the GR log responses increased to 240, 200-220, 220, and 220-240 gAPI, respectively, corresponding to more acidic rock composition, most likely igneous rock intrusions (andesite).

The SP log information indicates probable permeability potential in the well (Figure 22), which was seen in the following intervals: 1300-1304 m, 1403-1404m, 1408-1418 m, 1420-1428 m, 1488-1491, 1492.5-1495, 1501 -1506, 1517.5-1520, 1532-1543, 1557-1563, 1601-1605, and 1609-1613 m.

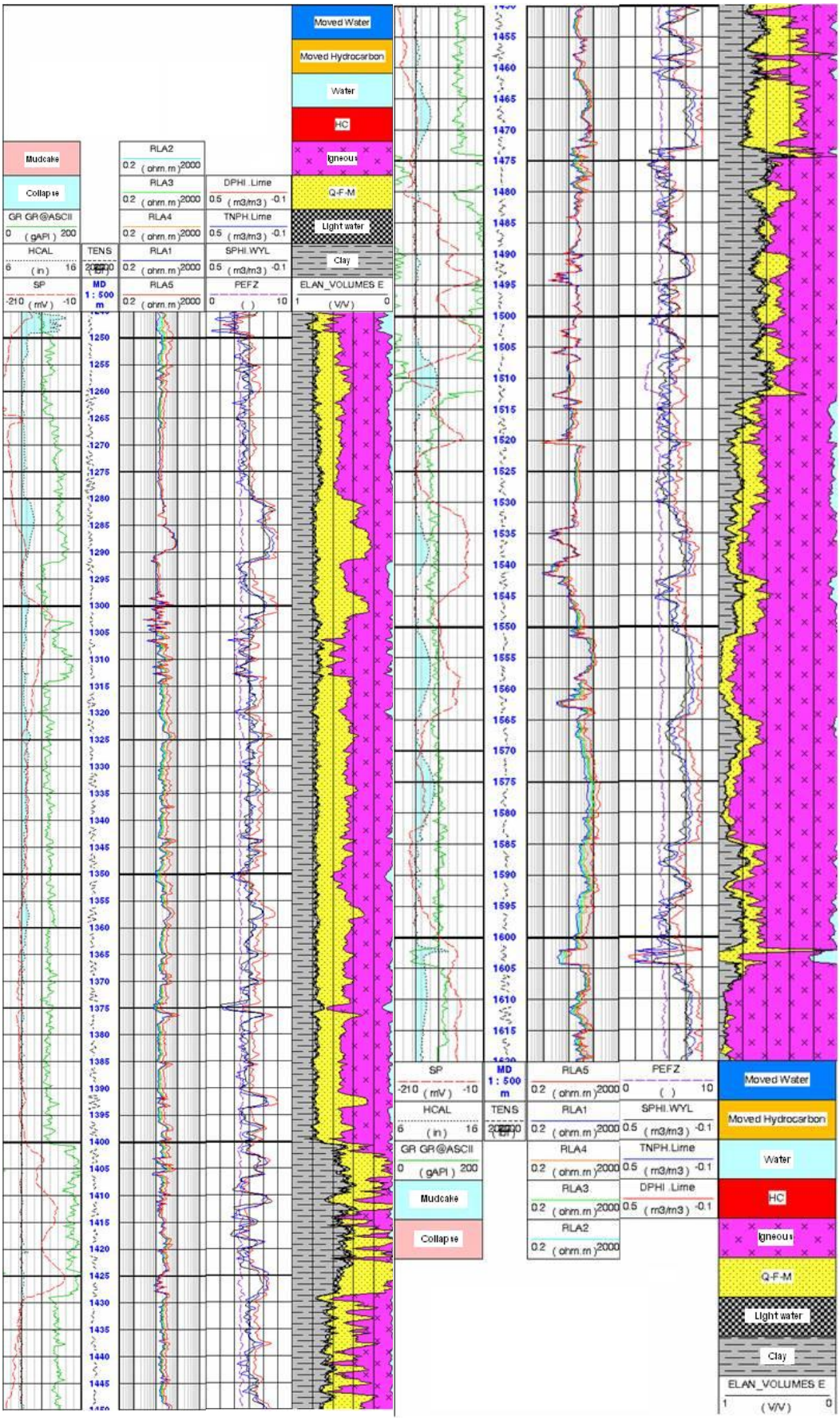

FIGURE 22*:* Lithological logs in well H-43 from the depth interval 1245-1625 m

In general, the most important permeable intervals in the recorded section are 1403-1428 and 1474-1512 m, where the first feed zone in the well was found.

The resistivity logs could indicate porous and/or permeable rock intervals by low resistivity reading with good log separation of the deep and shallow resistivity readings. Such low resistivity readings correspond to the interpretations of the drill-cuttings in the following intervals and points: 1492.5-1494, 1506, 1513, 1520, 1534 -1536, 1539-1542, 1561-1563 and 1601-1604 m. At these intervals and points, igneous rock is indicated (fractured andesite), see Figures 23 and 24 and Table 9. Based on this information, the intervals and points are in the same strata and show possible fracture zones.

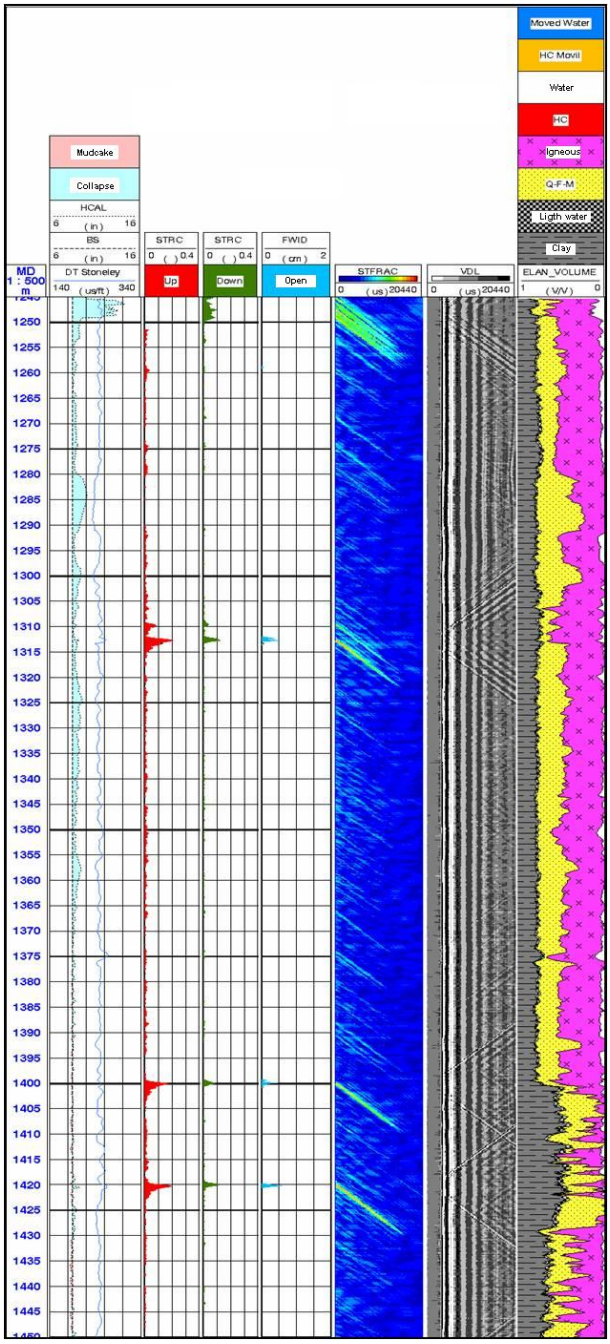

FIGURE 23: Full wave sonic interpretation of the fracture evaluation from the borehole Stoneley wave between 1245-1450 m in well H-43

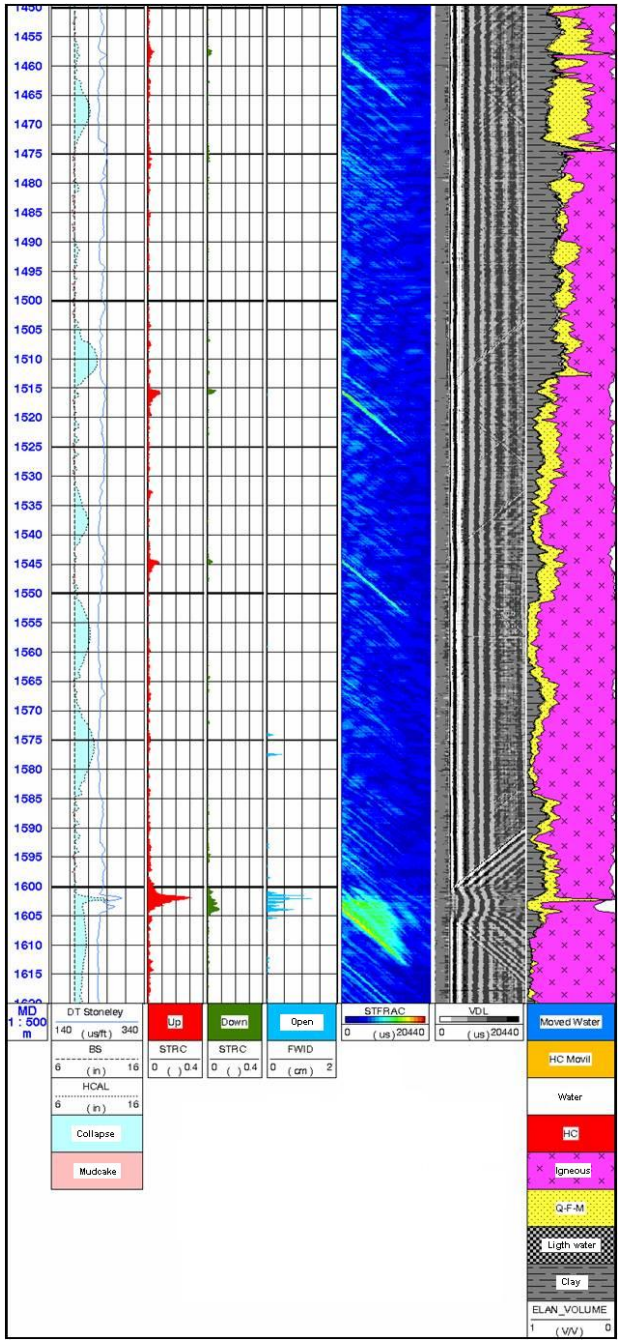

FIGURE 24: Full wave sonic interpretation of the fracture evaluation from the borehole Stoneley wave between 1450-1620 m in well H-43

TABLE 9: Possible fractures zones of well H-43

Intervals and points	Lithology	Full wave sonic log	Shear sonic imager log
1492.5 - 1494 m	Andesite		✓
1506 m	Andesite	✓	✓
1513 m	Andesite	✓	✓
1520 m	Andesite	✓	✓
1534 - 1536 m	Andesite		✓
1539 -1542 m	Andesite		✓
1561 - 1563 m	Andesite	✓	✓
1601 - 1604 m	Andesite	✓	✓

The Petrophysical analysis logs, e.g. density porosity, thermal neutron porosity, sonic porosity, etc. (see Table 5), obtained possible permeable zones (permeability may not always be present if you have high porosity, i.e. the rock may be porous but not necessarily permeable). These zones can be identified in Figure 22 at the following intervals and points: 1280-1290, 1298-1301, 1314, 1322, 1324-1325, 1334-1335, 1346, 1354-1358, 1365, 1376-1377, 1391-1393, 1397.5, 1403-1404, 1410-1412, 1420, 1424-1429, 1437.5, 1449-1452, 1455-1458, 1463-1474, 1490-1494, 1532-1543, 1548, 1552-1564, 1568-1585, 1590-1593, 1602, and 1605-1620 m.

The SonFrac fractures estimation log is derived from a full waveform analysis of an acoustic wave generated by a sonic tool in a borehole, producing both compression and shear waves. In addition, Stoneley waves can propagate along a solid-fluid interface, such as along the walls of a fluid-filled borehole and are the main low-frequency component of signals generated by sonic sources in boreholes. Analysis of Stoneley waves can allow the estimation of the locations of fractures and permeability of the formation (Schlumberger*, www.glossary.oilfield.slb.com)*. The other logs are displayed in Figures 23 and 24, lithology to the right, caliper log and bit size log both to the left. The SonFrac fractures estimation log shows the main open fracture and depth intervals.

The Dipole Shear Sonic Imager log combines monopole and dipole sonic acquisition capabilities. The transmitter section contains a piezoelectric monopole transmitter and two electrodynamic dipole transmitters perpendicular to each other. An electric pulse at sonic frequencies is applied to the monopole transmitter to excite compression- and shear-wave propagation in the formation. For Stoneley wave acquisition, a specific low-frequency pulse is used. The dipole transmitters are also driven at low frequency to excite the flexural wave around the borehole (Schlumberger, 2004a).

The Dipole Shear Sonic Imager logs (Figure 25) show the fractures and possible permeability within the following depth intervals:

- Interval 1601-1604 m: Strong signal change, visible fracture or bedding plane, possible permeability but no inflow into the well recorded.
- Intervals 1508-1510, 1516-1520, 1538-1540, 1542-1548, 1723-1727, 1737-1749, 1762.5-1765, and 1782.5-1800 m: Observed fractures or bedding planes (FMI), but no clearly visible permeability indications due to inflow into the well that could be confirmation from the temperature log analysis.

The other logs displayed in Figure 25 are: Poisson's ratio, compressional to shear velocity ratio, sonic porosity, gamma ray and, caliper. Table 10 summarises the information gathered on open fractures in well H-43.

TABLE 10: Main and secondary open fractures of well H-43

Open fracture	Depth intervals (m)
Main	1312-1315 1399-1401 1420-1421 1457-1459 1515-1516
Secondary	1245-1250 1544-1545 1601-1605

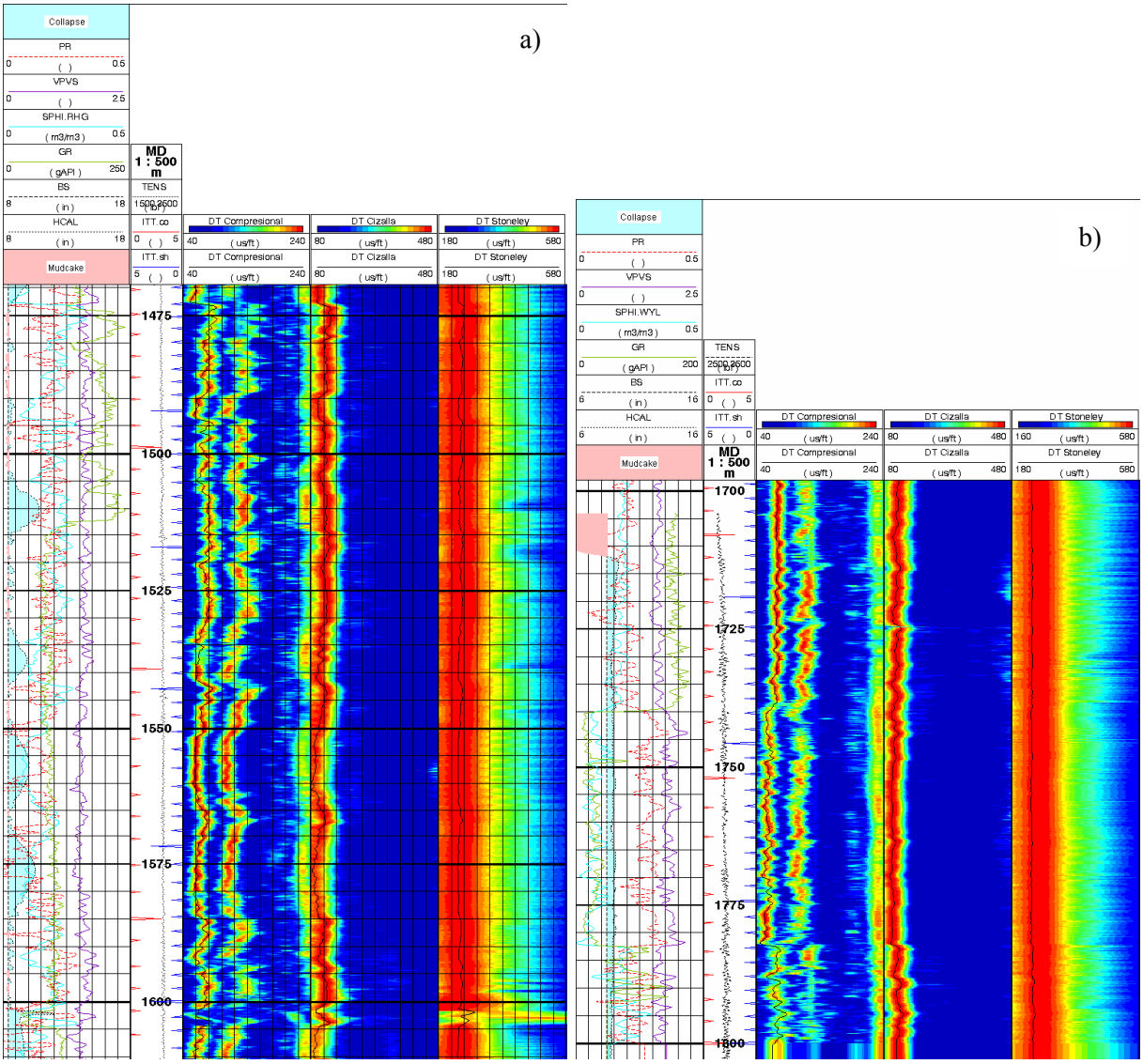

FIGURE 25: a) Dipole shear sonic imager interpretation of the fracture evaluation and permeability (mobility) from the borehole compression shear and Stoneley wave in well H-43
a) between 1470-1610 m; b) between 1700-1800 m

6.3 Fullbore formation microimage (FMI) logging

One of the objectives of the FMI log at well H-43 was to visualize whether the limestone was fractured and possibly permeable. The recordings were made by Schlumberger, on 10th January, 2008. Due to the high temperature recorded in well H-43, it was not possible to take the FMI to the bottom of the well, as the recording instruments only support a maximum temperature of 175°C. Two depth ranges were recorded, 1250-1633 and 1711-1813 m. The first interval did not present any problems during logging. However in the second interval, one of the 4 tool pads was damaged and did not provide complete recording.

6.3.1 Structural analysis of interval 1250-1633.5 m

In addition to the recording, the FMI was processed by Schlumberger; this report primarily uses the interpretations obtained by Schlumberger. The main objective was to identify areas of interest where the well intercepts the geothermal system in a fracturing-faulting zone, parallel to the primary strike

direction N-S of the Malpais and Antigua Faults zones which dip to the east. Moreover, it was important to identify and measure existing fractures and faults in the well by recording the azimuths of the strike direction that is orthogonal to dip direction (fault / fracture inclination). Figures 26-31 summarise the results of this.

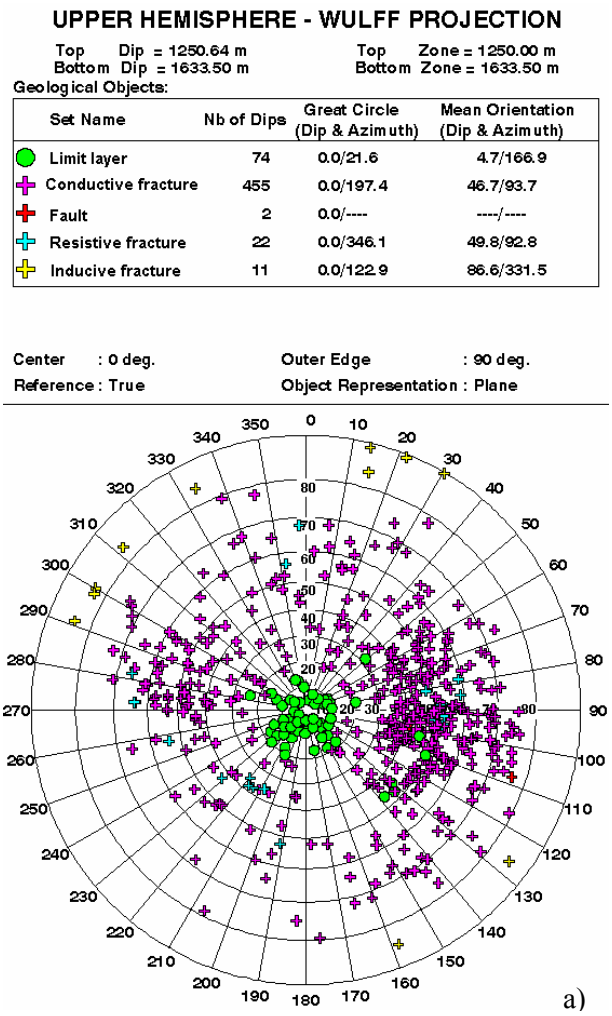

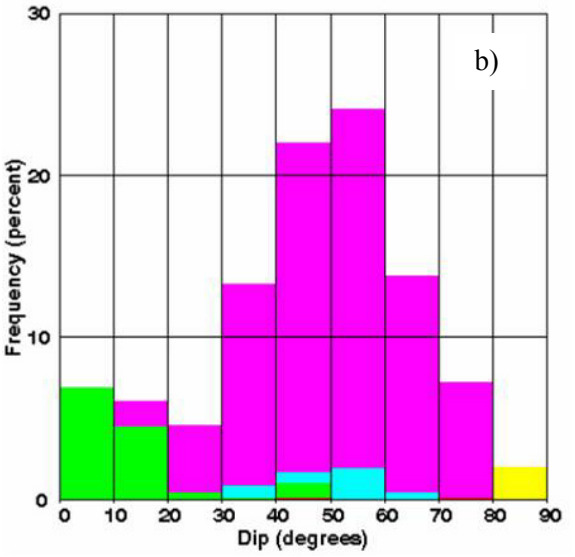

FIGURE 26: a) Stereonet of volcanic-lithology and b) histogram, interval 1250-1630 m of well H-43

Figure 26 shows a stereonet analysis (Wulff projection) and a fracture histogram. The stereonet structural analysis identifies maximum conductive fractures with the main orientation NNE-SSW and dip between 40 and 60 degrees. Only two faults with dip values between 70 and 80 degrees could be seen. The percentage of the main group of conductive faults in the well for this logging interval lies between 22 and 24%.

Figure 27 shows the strike and azimuth direction of the open fractures (conductive fractures) ranging from NW-SE to NE-SW. The most open fractures have strike direction NNE-SSW, with maximum dip in an ESE azimuth. Figure 28 shows the strike direction of the closed fractures (resistive fractures); the most vertical main strike direction is NNW-SSE with an easterly dipping azimuth. Figure 29 shows the strike and dip azimuth direction display of a fault, the main being NNE-SSW, and has an ESE dipping azimuth. Figure 30 shows the strike direction of the drilling induced fractures, which varies between the main directions from ENE-WSW to ESE-WNW.

The FMI image in Figure 31 shows the zone between 1310-1314 and 1398-1401 m, which appears to be an open fracture and bedding plane associated with a major wash-out. Although the logs give open fracture and possible bedding plane permeability indications, this zone was not related to any major inflow into the well; see temperature interpretations (Section 6.1).

Overall the interval 1250-1625 m is not very permeable in comparison to the main feed zone below 1950 m depth (see Section 6.1.2), which unfortunately could not be logged due to the high temperatures below 1815 m. The FMI instrument only supports temperatures up to 175°C.

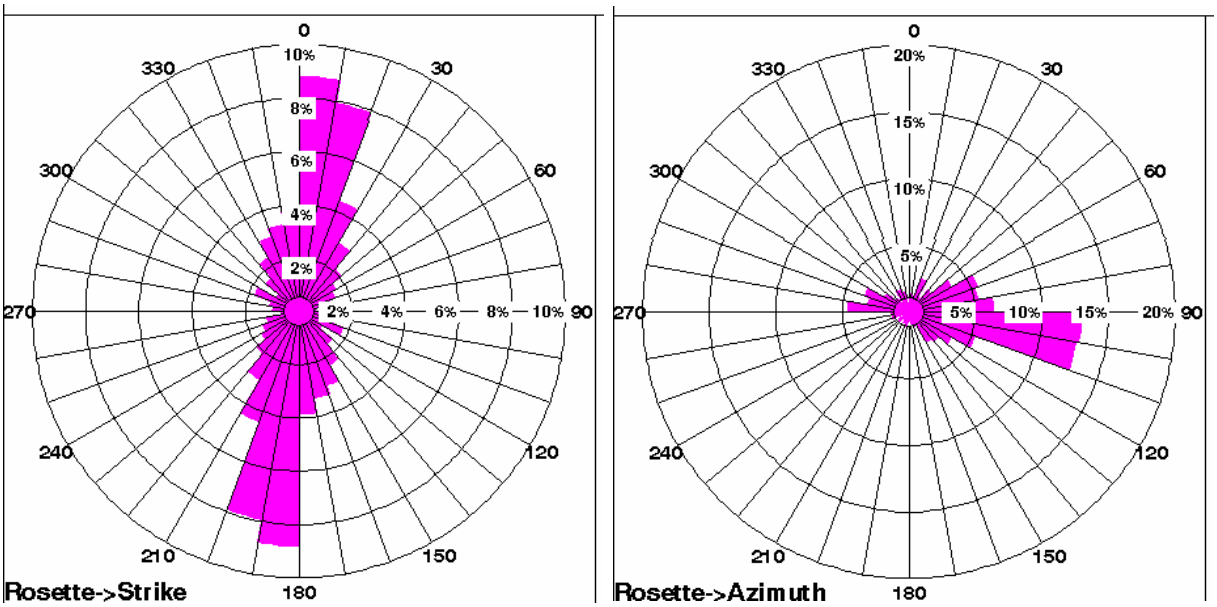

FIGURE 27: Strike and dip azimuth direction display of open fractures,
FMI interpretation of well H-43, interval 1250-1630 m

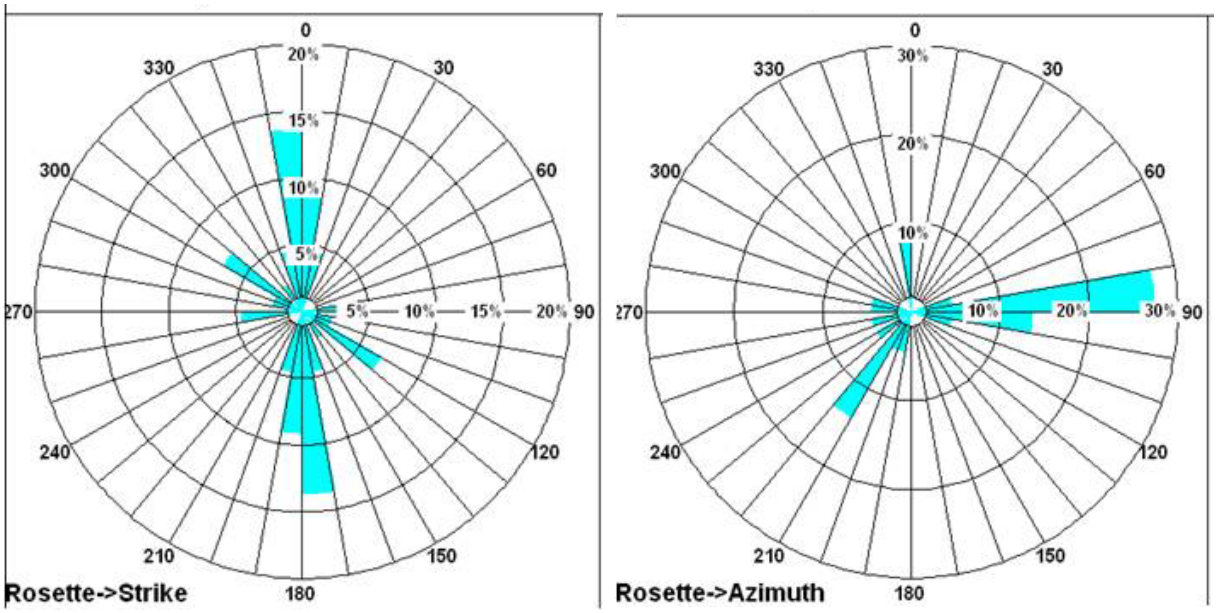

FIGURE 28: Strike and dip azimuth direction display of closed fractures,
FMI interpretation of well H-43, interval 1250-1630 m

6.3.2 Structural analysis: interval 1711-1813 m

The FMI log for this interval was recorded and processed by Schlumberger as well and interpretations by Schlumberger were used for this report. The second interval is in the depth range of 1711-1813 m. Figure 31 shows example cases observed on the FMI and the Borehole Stoneley wave interpretations.

Figures 32-36 summarise the results, with Figure 32 showing the Stereonet of fracture orientations and the same data in a histogram. The structural analysis presents maximum conductive fractures with a main SSW-NNE orientation and dip intervals between 30-40 degrees and 70-80 degrees. Nine faults with dip between 50 and 70 degrees can also be seen. Only three drilling-induced faults were recorded with fault dip values between 80 - 90 degrees. The percentage of conductive faults was about 10%.

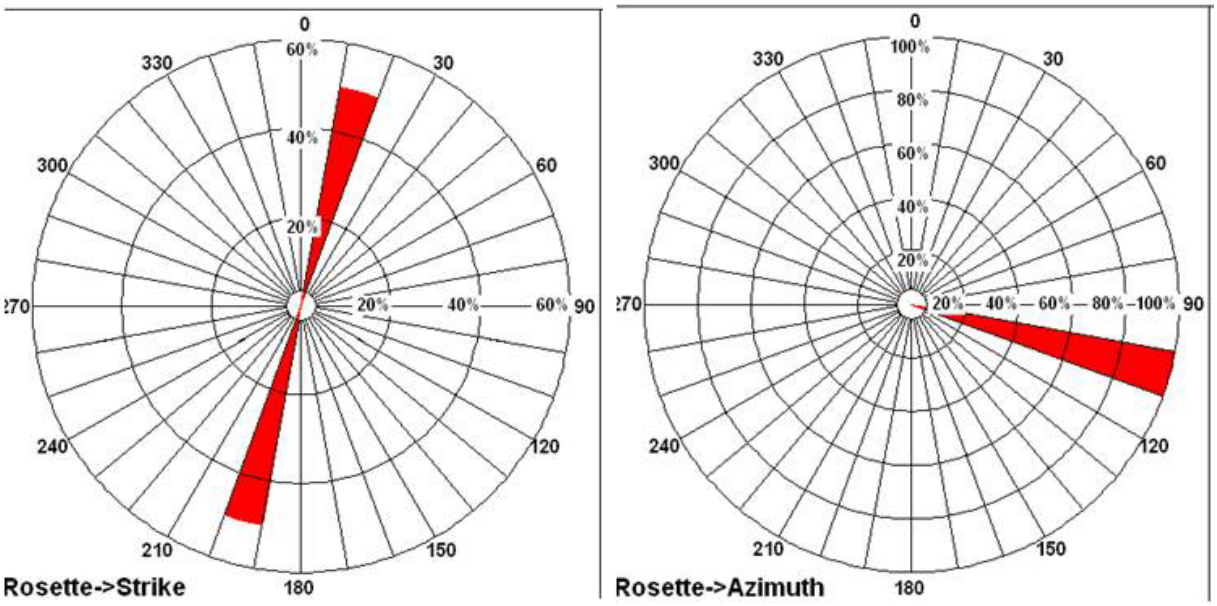

FIGURE 29: Strike and dip azimuth direction display of one fault, FMI interpretation of well H-43, interval 1250-1630 m

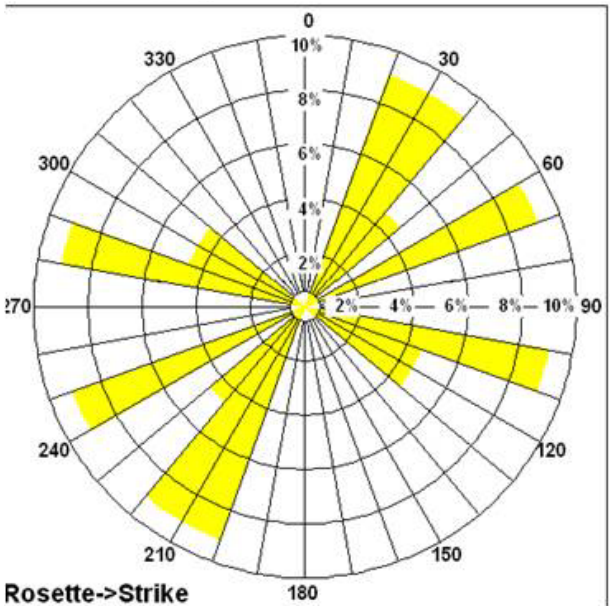

FIGURE 30: Strike direction display of drilling induced fractures derived from FMI interpretations of well H-43, interval 1250-1630 m

Figure 33 shows the strike and dip azimuth direction of the open fractures (conductive fractures); the main direction ranges from NW-SE to NE-SW with most open fractures striking N-S. Most conductive fractures appear to be dipping primarily due west. Figure 34 shows the strike and dip azimuth direction of the closed fractures (resistive fractures); the main strike direction here lies N-S and also W-E, respectively. Figure 35 shows the strike and azimuth direction display of a fault with a N-S strike direction and a dip azimuth due east. Figure 36 shows the strike direction display of the drilling-induced fracture and a main strike direction of NW-SE, which is in contrast with the N-S to NE-SW striking orientation of the open fracture and fault system in the shallower (1250-1633.5 m) logged section that appears to have a partially active open fracture fault system, which contributes to the inflow of the well.

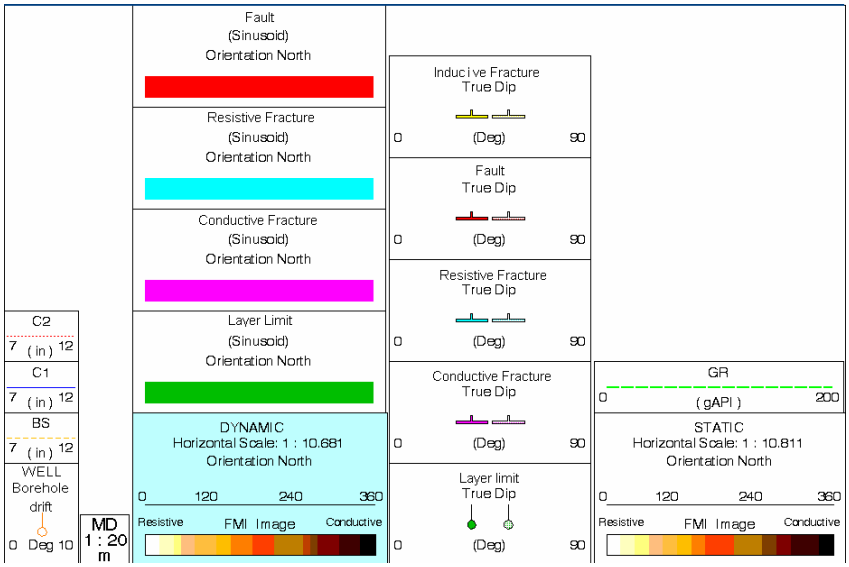

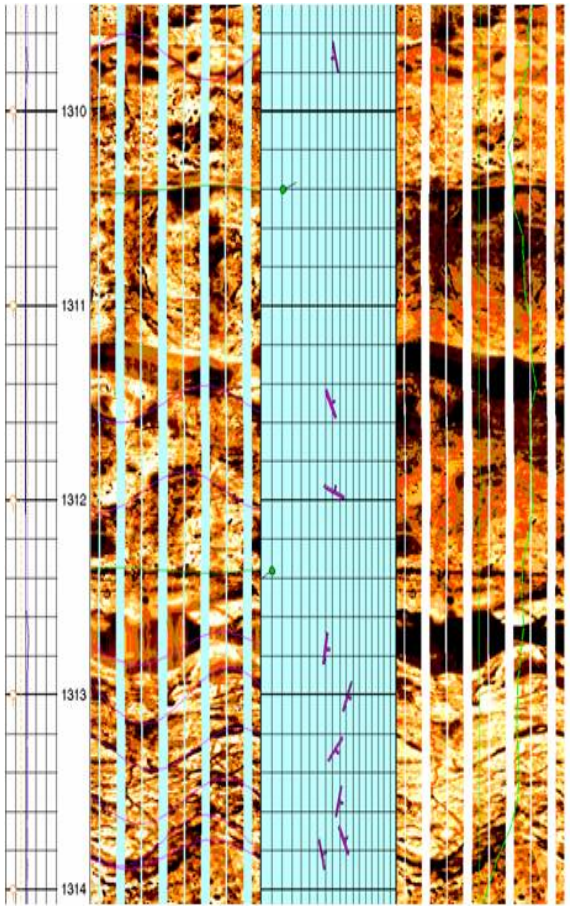

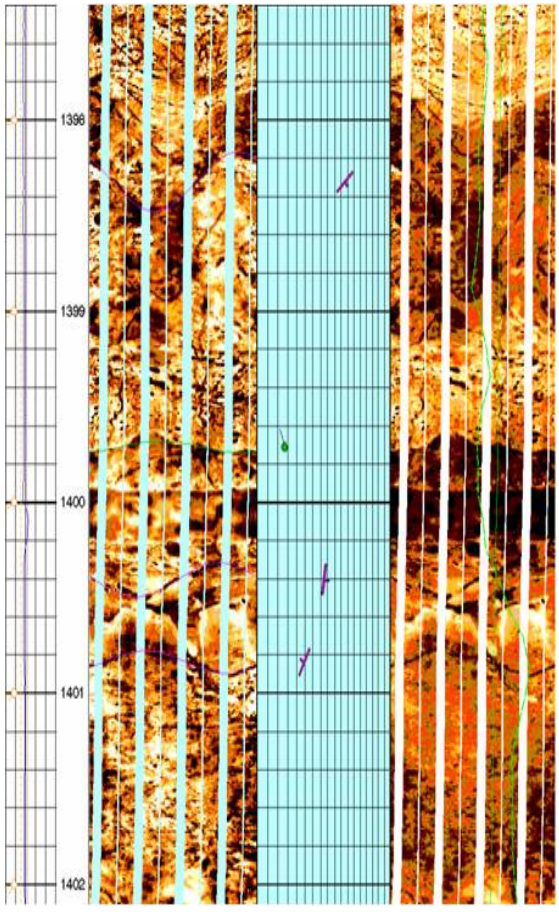

Open fracture zone around 1313 m indicated from the fracture evaluation of the borehole Stoneley wave interpretation	Open fracture zone around 1400 m indicated from the fracture evaluation of the borehole Stoneley wave interpretation (see Figure 25), appears more bedding plane connected / related

FIGURE 31: Example cases for open fracture / bedding plane interpretations that could be observed on the FMI and the borehole Stoneley wave interpretations between 1250 and 1625 m

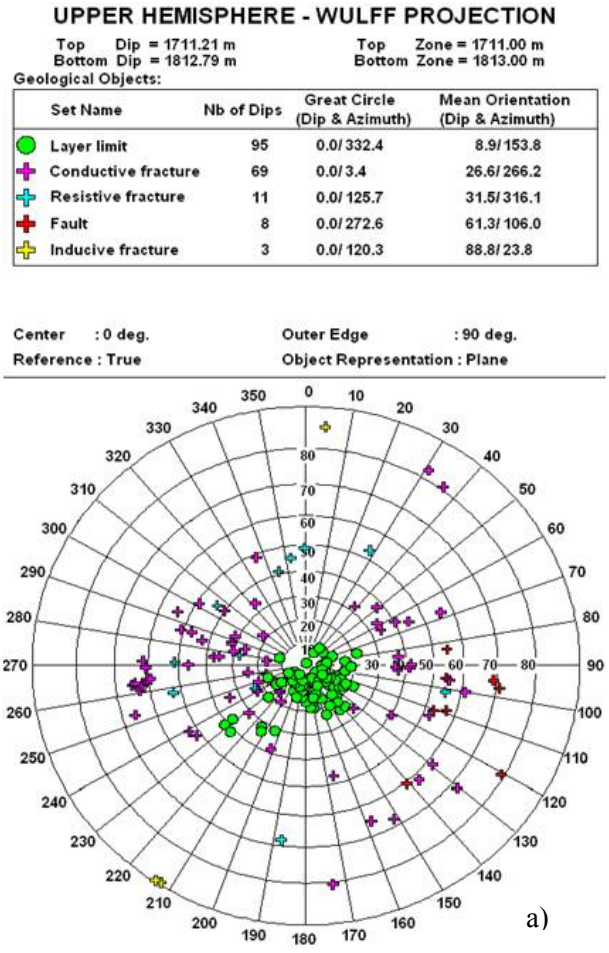

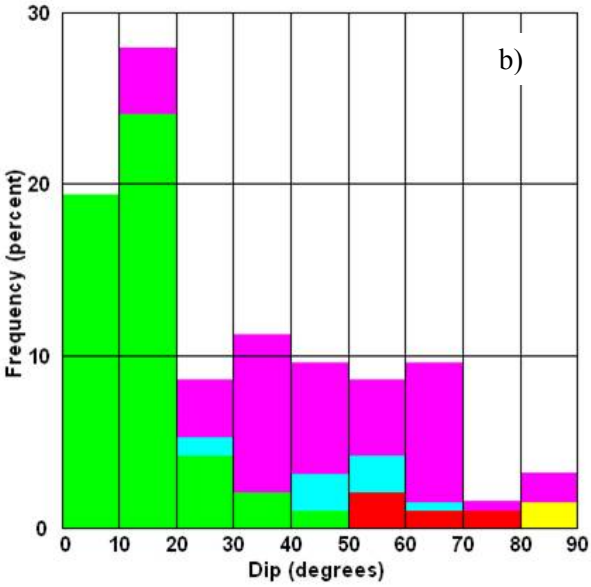

FIGURE 32: Stereonet of volcanic-lithology with red colour crosses indicating faults; the histogram shows the data between 1711 and 1813 m of well H-43

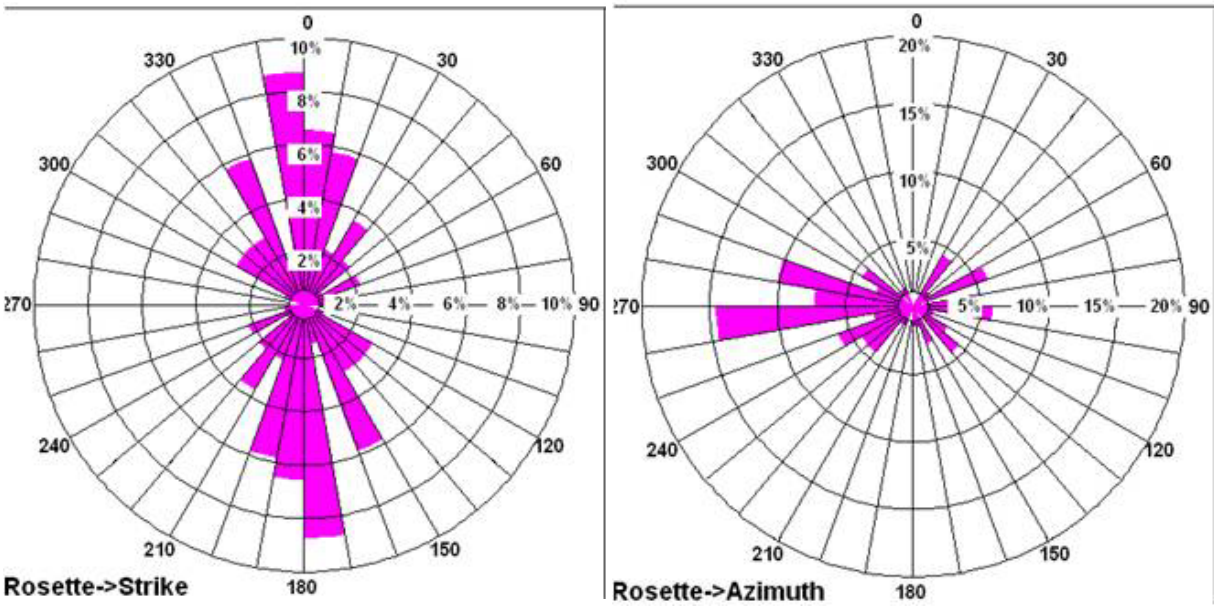

FIGURE 33: Strike and dip azimuth direction display of open fractures FMI interpretation of well H-43, interval 1711-1813 m

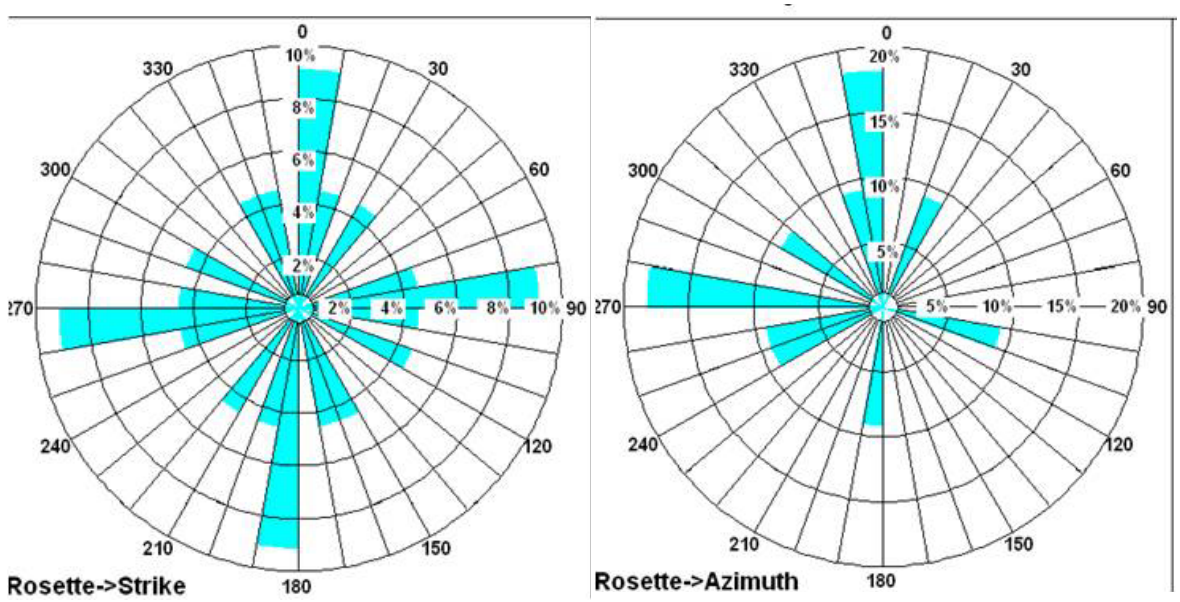

FIGURE 34: Strike and dip azimuth direction display of closed fractures,
FMI interpretation of well H-43, interval 1711-1813 m

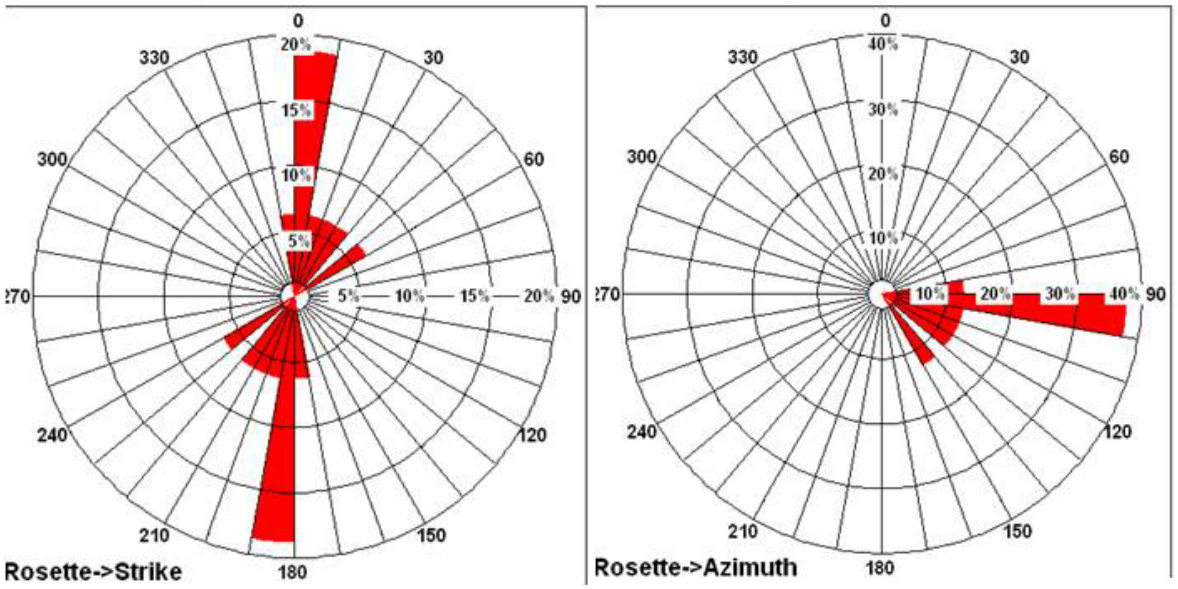

FIGURE 35: Strike and dip azimuth direction display of faults,
FMI interpretation of well H-43, interval 1711-1813 m

This logged section has to be described primarily as a tight section, with well visible bedding planes, possible intrusions, and some fractures that do not appear to contribute to inflow into the well, with reference to the temperature interpretation in Section 6.1, and the low response on the dipole shear sonic image interpretation (see Figure 25b) that indicated a rather tight hole for that deeper logged section. Due to the high temperature recorded in this well section, no SonFrac Fractures estimation log was performed (therefore, no velocity / Stoneley wave analysis for this section exists).

In Figure 37, the stress field interpretation of the tensile (drilling induced) fractures (yellow colour) indicates a 90° rotation to a NW-SE / W-E orientation right above the top basement, in comparison to the known stress field (maximum horizontal stress) orientation N-S to NE-SW in the shallower section of the volcanic deposits. The mapped open fractures and faults within the basement indicate again the primary N-S trend; in general, for fractures to be open, the minimum horizontal stress should be in a direction normal to the fracture plane (90° to the strike direction of a fracture/fault), therefore the fractures are not forced to be closed.

If this stress field change is correctly observed and not due to an interpretive error, then the fractures would tend to close in the traditionally known direction, explaining the rather tight well section for that deeper interval. To find an answer to this observation and stress field direction question, additional logging and interpretation of the FMI or even better, an acoustic borehole image logging and analysis in future wells should be conducted, focusing on the so-called basement interval as well. Traditionally, only the volcanic section has been logged.

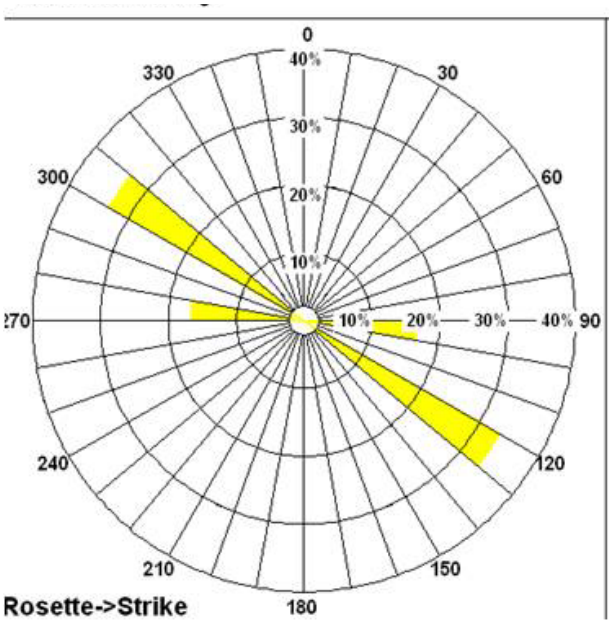

FIGURE 36: Strike direction display of drilling induced fractures, FMI interpretation of well H-43, interval 1711-1813 m

In addition to the regular borehole image analysis, it would be very important to conduct a stress field analysis of tensile fractures (drilling induced) and borehole breakouts. The interpretation by Schlumberger recorded only a few tensile fractures across a small depth range only. Here, it might be recommended to use an acoustic borehole imaging tool that would focus on the open fracture and fault zones but would not map all fractures (open and closed), fault and bedding features. For a better comparison and explanation, see Section 6.4 below.

6.4 Comparison of acoustic and electrical image logs

The Formation Micro Scanner logs (FMS) generally reveal more planar structures than Borehole Televiewer (BHTV) logs and are sensitive to characteristics like foliation, layering, or systematic variations in resistivity related to mineralogy or fluids. More than 50% of the planar structures are imaged by FMS logs. These fabric elements probably do not contribute to reservoir productivity. In contrast, BHTV logs preferentially record open or un-cemented fractures that are more likely to break the continuity of the borehole wall; thus, it is unlikely to image fabric. As a result, FMS logs may provide a more complete record of the entire fracture population, possibly including healed fractures and foliation, while BHTV logs more selectively image "open" natural fractures that are expected to contribute to reservoir permeability.

High-temperature instruments (comparison)
The Schlumberger Fullbore Formation MicroImager (FMI) instrument was not taken any deeper in well H-43 because of its temperature limitation (approx. 150°C, max. 177°C) (Schlumberger, 2004b). This is a common limitation of geophysical borehole instruments. Steps are however being taken to improve the situation, allowing wireline logging at higher temperatures than previously possible. The ABI85 borehole televiewer from Advanced Logic Technology (ALT) is a very good example of a high-temperature wireline logging instrument, capable of 12 hour operation at +275°C (excursions to +300°C) (Davatzes, 2007).

Faults and fractures in image logs
Figure 38 shows an example of recorded use of BHTV and FMS measurement instruments (obtained from Davatzes, 2007). The BHTV shows clear and complete information on faults and fractures in the well, in contrast with FMS, with four Pads giving information in vertical non-continuous sections, losing potentially important values needed for interpretation. *The following remarks can be given* (Davatzes, 2007):

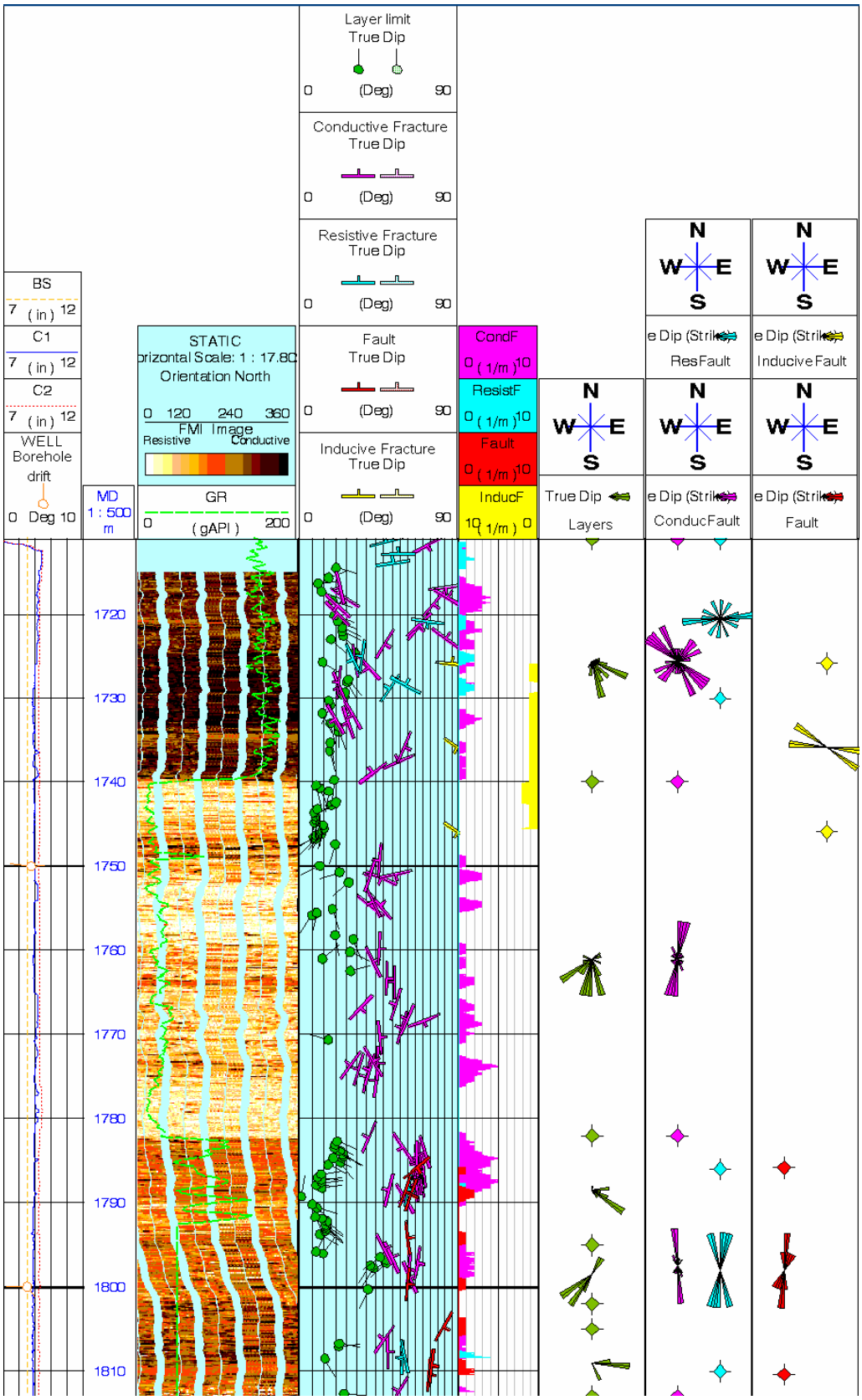

FIGURE 37: Example cases for open fracture, closed fracture, induced fracture and fault interpretations that could be observed on the FMI between 1711 and 1813 m; an open fracture zone is found around 1711-1740 m; a closed fracture zone mixed interval is between 1720 and 1730 m; and a fault zone around 1782-1813 m

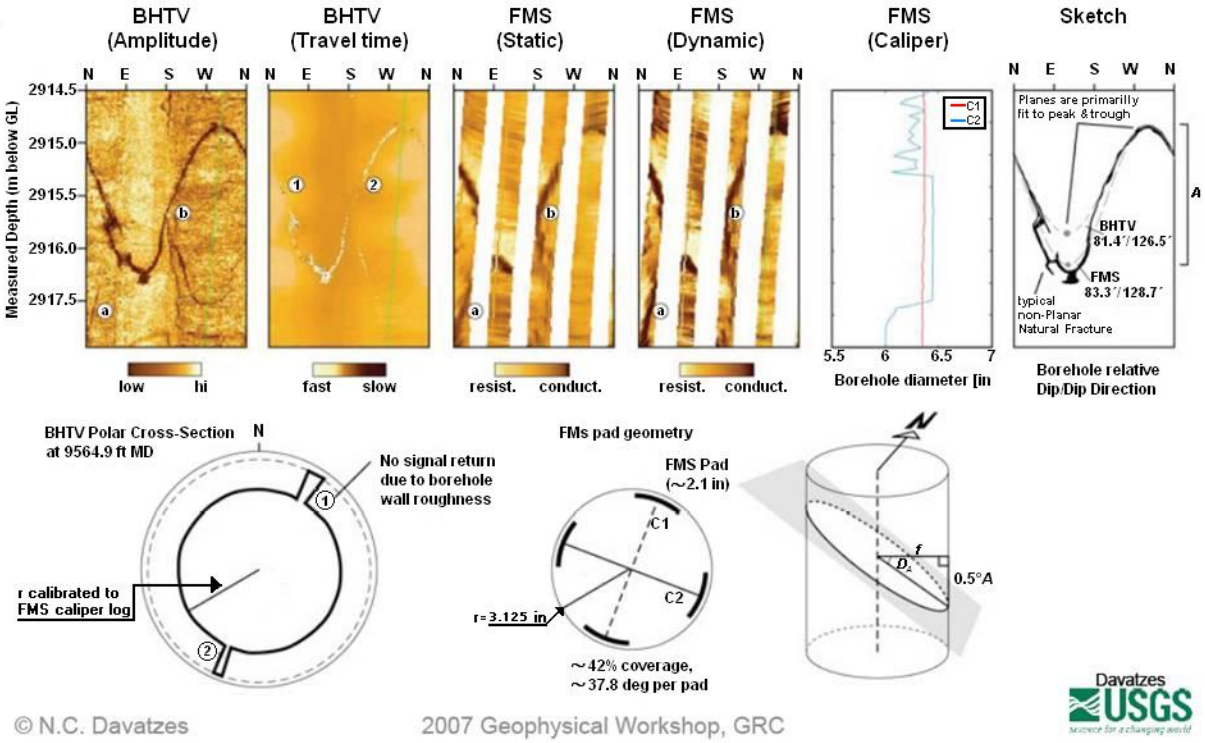

FIGURE 38: Example of comparison results obtained between BHTV and FMS (by Davatzes, 2007)

- Image logs probably provide the highest resolution characterisation of the borehole logs.
- Fracture orientations can be measured in image logs.
- BHTV preferentially images open fractures, whereas electrical resistivity logs image both "healed" and open fractures (these logs provide complementary insights into fracture properties because they measure different physical properties).
- Image logs estimate fracture density.

Nevertheless, even though BHTV logs give an "incomplete" picture of the fault / fracture system in a borehole, a combination of the FMI and BHTV, especially during the exploration / research stage of an area, would give a complete understanding of the fault / fracture system (closed and open) and differentiate the open fracture system with the BHTV. During routine production drilling and logging, the use of the BHTV is commonly applied to track the open fractures and faults in relation to open feed zones / reservoirs.

7. HITI PROJECT AND THE IDDP

The HITI project is an on-going research and development project funded within the 6th European research framework program and deals with the analysis of hot and corrosive supercritical geothermal reservoirs using new high-temperature instruments being developed within the project (HITI stands for 'High-temperature instruments for supercritical geothermal reservoir characterisation and exploitation'). It would have been very useful, for geophysical characterisation of well H-43, to have access to these new instruments, since the temperatures in H-43 are very high and it has acidic fluids.
In March 2008, temperature and pressure measurements were recorded in well H-43 (Figure 39). The maximum temperature recorded at the bottom of the well (2200 m) was 395.4°C at a pressure of 112.74 kg/cm^2. These conditions are already at the upper limit of conventional high-temperature logging instruments and actually beyond the range of any borehole instruments other than special

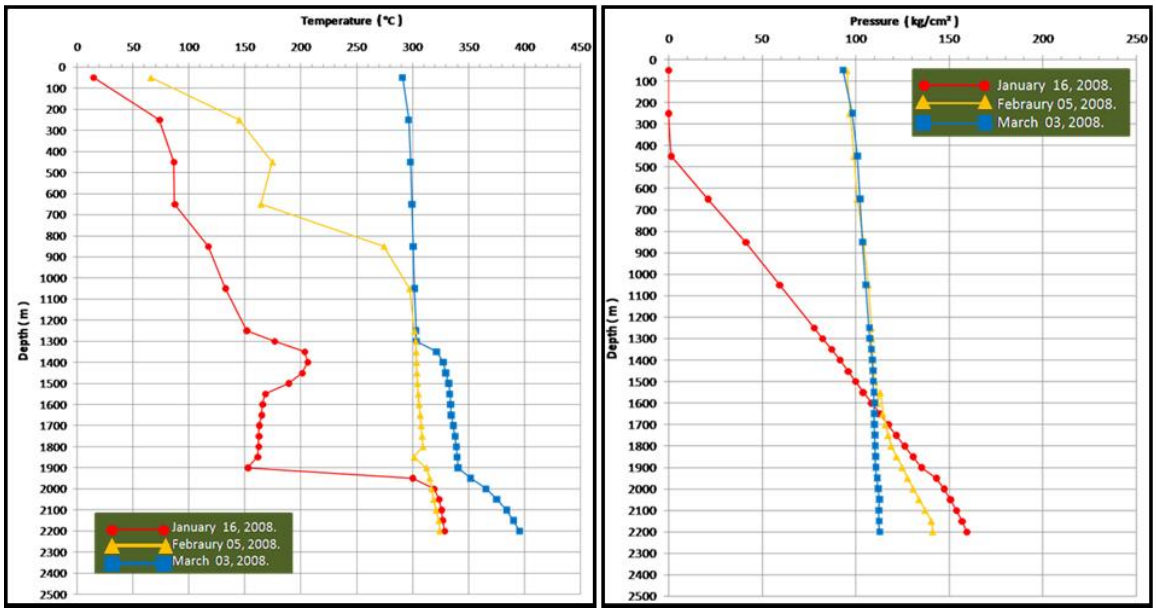

FIGURE 39: Temperature and pressure logs from well H-43, red colour after thermal breakthrough, yellow and blue colours after heating of the well

temperature and pressure gauges. The measured maximum temperature of well H-43, after heating up, is similar to the calculated extrapolated Horner temperature, i.e. 383°C at 2200 m depth (see Section 6.1). The final temperature at 2200 m depth is well above the supercritical point of water 374.15°C, but the pressure does not correspond to that water phase (should be above 224 kg/cm^2).

8. CONCLUSIONS AND RECOMMENDATIONS

Research and analysis results of well H-43 have led to the following conclusions:

- ✓ Well H-43 presents two feed zone intervals:
  - Secondary zone at 125-1550 m depth in andesite layer (igneous rock);
  - Main zone at 1950-2200 m depth in fractured limestone.
- ✓ Well H-43 has the following specifications:
  - Highest temperature after thermal breakthrough was 328.64°C;
  - Highest temperature after heating 395.4°C;
  - Pressure after thermal breakthrough 159.34 kg/cm^2;
  - Pressure after heating 112.74 kg/cm^2;
  - Depth of the well is 2200 m.
- ✓ Well H-43 is acidic, the pH during drilling shows basic values 12-8, but after cleaning and heating of the well, pH value lowered to 5.34. Work on neutralizing acidic fluids is ongoing.
- ✓ The FMI analysis shows layer limit, conductive, resistive and inductive fractures and faults.
- ✓ The conductive fractures have main dip values between 40 and 60°; the preferential strike directions are N-S to NNE-SSW.
- ✓ The resistive fractures have main dip values between 50 and 60°; the preferential strike direction is NNW-SSE to N-S and E-W.
- ✓ The identified faults have preferential strike directions of NNE-SSW and N-S; the dip values are between 50 and 80°. Major faults recorded within the deeper data coverage between 1782-1813 m could be related to micro-seismicity that was recorded as well, indicating the presence of stress release but with no direct indication of permeability for that logged interval.
- ✓ The deepest interval of the well, below 1813 m, with the main feed zone below 1950 m, has not been logged due to temperature restrictions of the logging tools.
- ✓ Well H-43 is more powerful than any other well in the field (see Table 11).

TABLE 11: Offset well comparison for well H-43

Well	Temperature (°C)	Depth (m)	Q (tons/h)	Feed zones intervals in md (m)	
H-3D	219	1860	7.70	1225 - 1325	1425 - 1500
H-9	255	2500	49.21	1700 - 2000	2100 - 2400
H-16	203	2048	10.9	1480 - 1660	1745 - 1960
H-33	218	1600	11.67	1100 - 1350	1500 - 1600
H-35	235	1690	43.30	1250 - 1300	1350 - 1450
H-37D	233	1705	33.65	1350 - 1450	1500 - 1570
H-43	**395.4**	**2200**	**51.95**	**1250 - 1550**	**1950 - 2200**

Source: Los Humeros geothermal field and sub-management of studies, Morelia

The research, analysis and understanding of high-temperature well H-43 leads to the following recommendations for future work in the area:

- ✓ In well H-43 the main feed zone lies within the faulted and fractured limestone formation between 1950 m and 2200 m. Geophysical logs should be run to this depth, and information obtained on conditions at the bottom of the well; this may be possible if higher temperature tolerant instruments become available (e.g. such as those being developed in the HITI Project).
- ✓ Perform BHTV logging in the future, due to their focus on "open" natural fractures that are expected to contribute to reservoir permeability. Such an instrument is now capable of 12 hour operation at +275°C (possibly up to +300°C).
- ✓ Conduct a 3-D structural and stress field analysis for the volcanic belt and the basement section to obtain a better understanding of the tie-in of seismicity data across the field.

ACKNOWLEDGEMENTS

I would like to express my gratitude to the United Nations University and to the Government of Iceland for giving me the chance to participate in the Geothermal Training Programme in Iceland. I would also like to express my thanks to Dr. Ingvar B. Fridleifsson, Mr. Lúðvík S. Georgsson, Ms. Thórhildur Ísberg, Mrs. Dorthe H. Holm, and Mr. Markús A.G. Wilde. I sincerely thank my supervisors, Ragnar K. Ásmundsson and Anett Blischke, for the long hours and dedication in guiding me during this project. I wish to express my sincere gratitude to the Gerencia de Proyectos Geotermoelectricos (C.F.E) for the chance and support to participate in this training. Also I thank Mr. Raúl Maya, Mr. Magaly Flores and the entire geothermal staff for their support during my preparation for the course and report. My deepest gratitude goes to my family for their moral and emotional support during these six months. Thank you, my husband Daniel, for your support and understanding.

REFERENCES

Antayhua, Y., 2007: *Seismicity of the Los Humeros-Puebla geothermal field (1997-2004), its relationship with the local wells and tectonics* (in Spanish). Universidad Nacional Autónoma de México, Posgrado en Ciencias de la Tierra, MSc thesis, 136 pp.

Arellano, M., García, A., Barragán, M.R., Izquierdo, G., Aragón, A., and Pizano, A., 2000: *Initial distribution of pressure and temperature of the Los Humeros geothermal field* (in Spanish). Boletín Instituto de Investigaciones Eléctricas – Comisión Federal de Electricidad, Mexico, 450 pp.

Ascencio, F., García, A., Rivera, J. and Arellano, V., 1994: Estimation of undisturbed formation temperatures under spherical-radial heat flow conditions. *Geothermics, 23-4*, 317-326.

Boyle, K., Hutchings, L., Bonner, B., Foxall, W., and Kasameyer, P., 2007: *Double difference earthquake locations at the Salton Sea geothermal reservoir*. Lawrence Livermore National Laboratory (LLNL), Livermore, CA, 12 pp.

Cedillo, F., 1997: *Surface geology of the Los Humeros geothermal field* (in Spanish). Comisión Federal de Electricidad – Gerencia de Proyectos Geoterrmoeléctricos, Los Humeros, report HU/RE/03/97.

Davatzes, N., 2007: *Logging tools for fracture characterization, stress analysis, and permeability evolution: Image log interpretation*. Geothermal Resources Council, Geophysical Workshop, 54 pp.

Doveton, J.H., and Prensky, S.E., 1992: Geological applications of wireline logs a synopsis of developments and trend. *The Log Analyst, 33,* 286-303.

Dowdle, W. L., and Cobb, W.M., 1975: Static formation temperature from well logs - an empirical method. *J. Petroleum Technology, 27,* 1326-1330.

Lashin, A., 2005: Reservoir parameter estimation using well logging data and production history of the Kaldárholt geothermal field, S-Iceland. Report 12 in*: Geothermal training in Iceland 2005*. UNU-GTP, Iceland, 163-200.

Lermo, J., 1999: *Earthquake of the Los Humeros, Puebla, on November 25th 2004 (Mc=4.6) and its relationship to the geothermal field* (in Spanish). Instituto de Ingeniería, Mexico, informal report, 60 pp.

Lermo J., Lorenzo, C., and Espitia, G., 2006: *Seismic activity of the Los Humeros, Puebla geothermal field* (in Spanish). Comisión Federal de Electricidad, Gerencia de Proyectos Termoeléctricos-Departamento de Exploración. technical report GF-HU-01-06, 58 pp.

Negendank, J.F.W., Emmermann, R., Krawczyk, R., Mooser, F., Tobschall, H., and Werle, D., 1985: Geological and geochemical investigations on the eastern Trans-Mexican volcanic belt. *Geof. Internac.*, 24, 477-575.

Palma, S., 2007: *Analysis of TDEM and proposal for drilling in Los Humeros, Puebla* (in Spanish). Comisión Federal de Electricidad, report GF-HU-08-07, 13 pp.

Rocha, S., Jimenez, E., and Arredondo, J., 2006: *Proposal for back-up wells for the Los Humeros geothermal field: H-41, H-42 and H-43* (in Spanish). Comisión Federal de Electricidad, report OGL-HM-01/06, 34 pp.

Sánchez, M., and Torres, R., 2008: *Analysis and diagnosis of tests during drilling of well H-43 in the Los Humeros, Puebla geothermal field. Analysis of steam requirements DINYAC-007-2008* (in Spanish). Comisión Federal de Electricidad, report *RC-SDE-005*, 23 pp.

Schlumberger, 2004a: *DSI dipole shear sonic imager*. Schlumberger, report, August, 2 pp.

Schlumberger, 2004b: *FMI fullbore formation microimager*. Schlumberger, report, August, 2 pp.

Stefánsson, V. and Steingrímsson, B., 1990: *Geothermal logging I: An introduction to techniques and interpretation* (3rd edition). Orkustofnun, Reykjavík, report OS-80017/JHD-09, 117 pp.

Viggiano, J., and Flores, M., 2008: *Petrographic studies of well H-43, the Los Huemros geothermal field: Interpretation and mineralogical indicators of acidity* (in Spanish). Comisión Federal de Electricidad, report, 30 pp.